Constrained Aero-elastic Multi-Point Optimization Using the Coupled Adjoint Approach

M. Abu-Zurayk

MUSAF II Colloquium

20th Sept. 2013, Toulouse

DLR

Table of Contents

- Motivation
- Formulation of the Coupled Adjoint Approach
- Test Case Description
- Unconstrained Single-Point Optimization
- Constrained Single- and Multi-Point Optimizations
- Future Work: Gradient Correction due to Trimming
- Conclusions

Motivation

- During the flight, the wing deforms due to the aero-elastic effects.
- The aero-elastic deformation significantly modifies the wing shape (twist and bending) and impacts the aerodynamic coefficients => need to take them into account in the design phase.

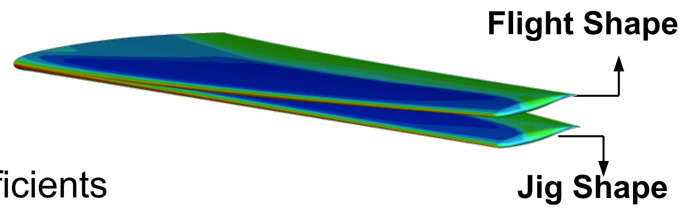

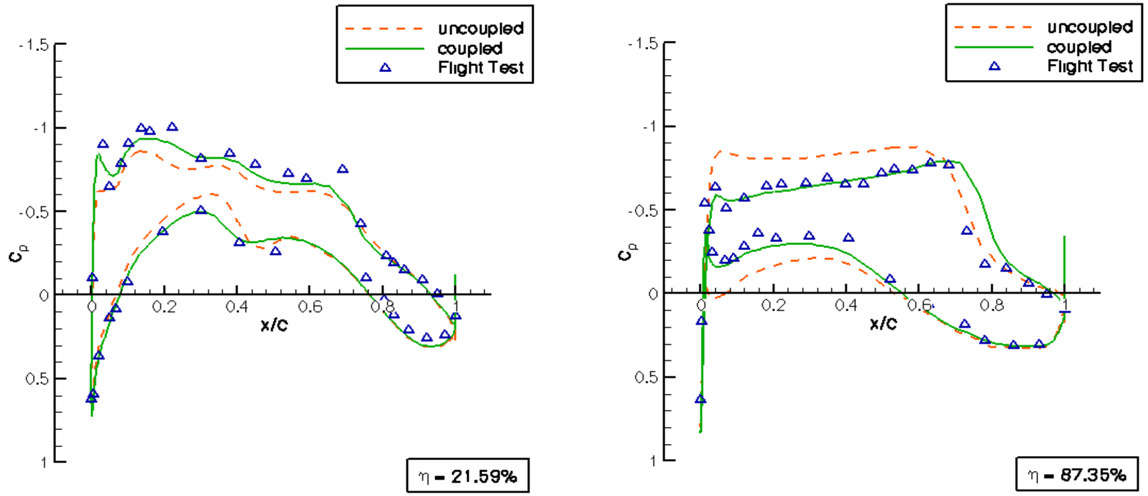

Courtesy of Stefan Keye

Motivation

- During the flight, the wing deforms due to the aero-elastic effects.
- The aero-elastic deformation significantly modifies the wing shape (twist and bending) and impacts the aerodynamic coefficients => need to take them into account in the design phase.

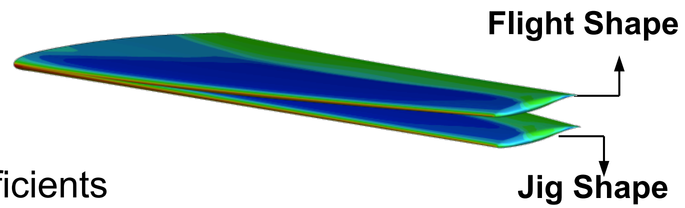

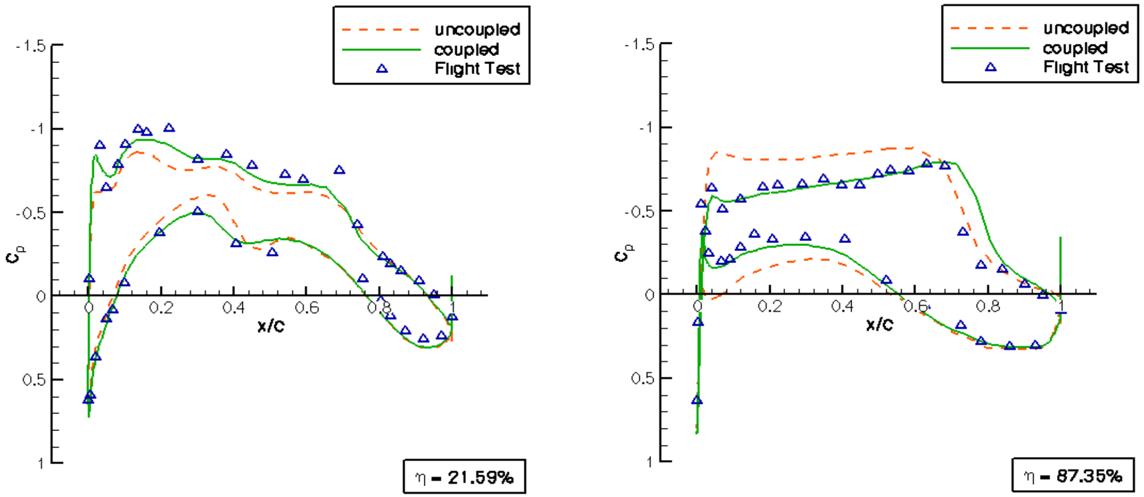

Courtesy of Stefan Keye

The effect becomes more evident towards the wing tip

Motivation

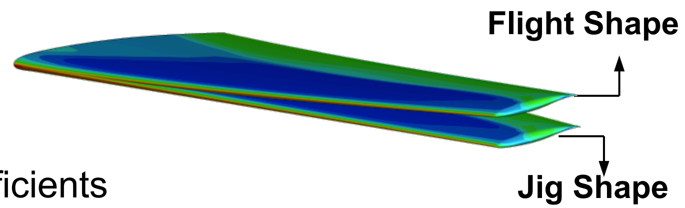

- During the flight, the wing deforms due to the aero-elastic effects.
- The aero-elastic deformation significantly modifies the wing shape (twist and bending) and impacts the aerodynamic coefficients => need to take them into account in the design phase.

- Several approaches for dealing with elasticity in wing design

Motivation

- During the flight, the wing deforms due to the aero-elastic effects.
- The aero-elastic deformation significantly modifies the wing shape (twist and bending) and impacts the aerodynamic coefficients => need to take them into account in the design phase.

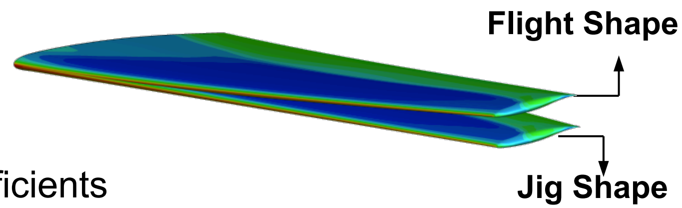

- Several approaches for dealing with elasticity in wing design

1. Stiffer wing reduces the deformation (elastic effects)

Motivation

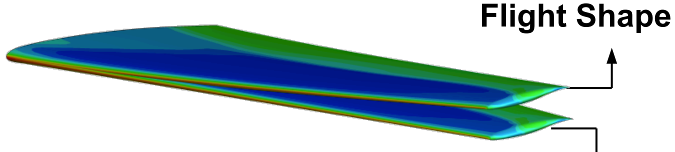

- During the flight, the wing deforms due to the aero-elastic effects.
- The aero-elastic deformation significantly modifies the wing shape (twist and bending) and impacts the aerodynamic coefficients => need to take them into account in the design phase.

- Several approaches for dealing with elasticity in wing design

1. Stiffer wing reduces the deformation (elastic effects) …. BUT this increases the weight

Motivation

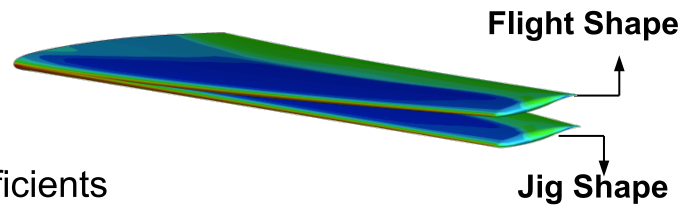

- During the flight, the wing deforms due to the aero-elastic effects.
- The aero-elastic deformation significantly modifies the wing shape (twist and bending) and impacts the aerodynamic coefficients => need to take them into account in the design phase.

- Several approaches for dealing with elasticity in wing design

1. Stiffer wing reduces the deformation (elastic effects) …. BUT this increases the weight
2. Design the *Fight shape* and inversely compute the *Jig shape*

Motivation

- During the flight, the wing deforms due to the aero-elastic effects.
- The aero-elastic deformation significantly modifies the wing shape (twist and bending) and impacts the aerodynamic coefficients => need to take them into account in the design phase.

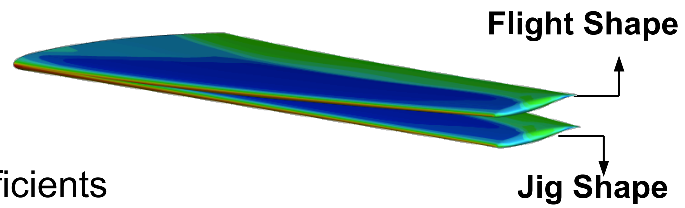

- Several approaches for dealing with elasticity in wing design

1. Stiffer wing reduces the deformation (elastic effects) …. BUT this increases the weight
2. Design the *Fight shape* and inversely compute the *Jig shape* …. Requires experience

…. What about multipoint ?

Aeroelastic deformation is dependent on the flow condition (Mach, lift,…)

Motivation

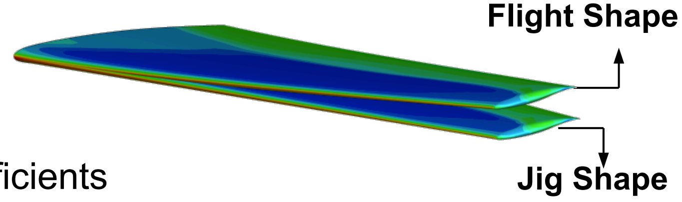

- During the flight, the wing deforms due to the aero-elastic effects.
- The aero-elastic deformation significantly modifies the wing shape (twist and bending) and impacts the aerodynamic coefficients => need to take them into account in the design phase.

- Several approaches for dealing with elasticity in wing design

1. Stiffer wing reduces the deformation (elastic effects) …. BUT this increases the weight
2. Design the *Fight shape* and inversely compute the *Jig shape* …. Requires experience
   …. What about multipoint ?
   Aeroelastic deformation is dependent on the flow condition (Mach, lift,…)
3. Start with *Jig shape* and design *Flight shape*

Motivation

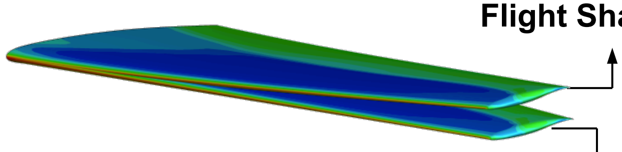

- During the flight, the wing deforms due to the aero-elastic effects.
- The aero-elastic deformation significantly modifies the wing shape (twist and bending) and impacts the aerodynamic coefficients => need to take them into account in the design phase.

- Several approaches for dealing with elasticity in wing design

1. Stiffer wing reduces the deformation (elastic effects) …. BUT this increases the weight
2. Design the *Fight shape* and inversely compute the *Jig shape* …. Requires experience
   …. What about multipoint ?
   Aeroelastic deformation is dependent on the flow condition (Mach, lift,…)
3. Start with *Jig shape* and design *Flight shape* …. Works for multipoint. However, requires coupled CFD-CSM simulations

Motivation

- The aero-elastic equilibrium is obtained after several couplings between aerodynamics and structure and incurs high-computational cost
  => in case of optimization efficient strategies are required

.

.

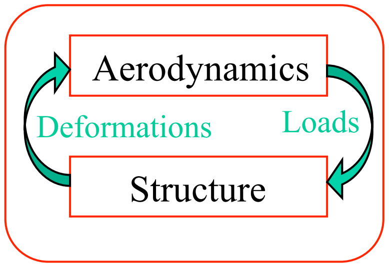

Motivation

- The aero-elastic equilibrium is obtained after several couplings between aerodynamics and structure and incurs high-computational cost
  => in case of optimization efficient strategies are required

- Gradient-based optimization algorithms are known to be efficient but computing the gradients is expensive with the standard finite differences approach.

.

Traditional Finite Differences Approach

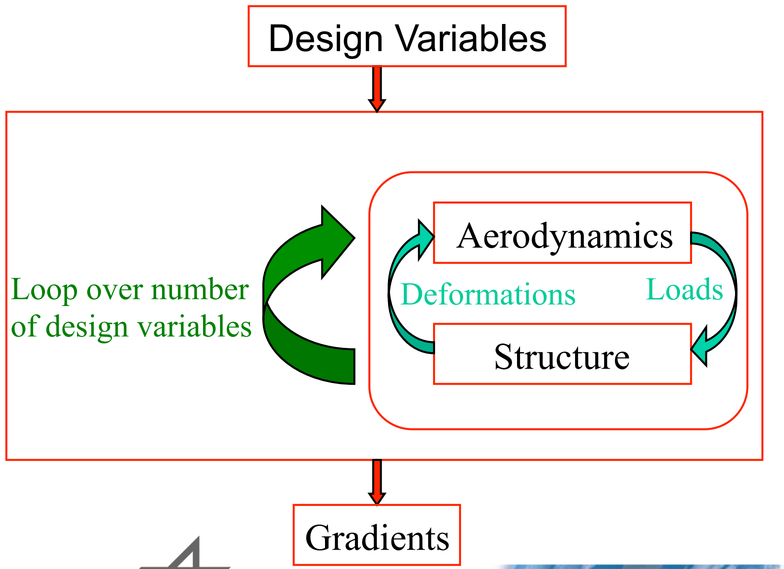

Motivation

- The aero-elastic equilibrium is obtained after several couplings between aerodynamics and structure and incurs high-computational cost
  => in case of optimization efficient strategies are required

- Gradient-based optimization algorithms are known to be efficient but computing the gradients is expensive with the standard finite differences approach.
  => need for an efficient approach to determine the gradients: the coupled aero-structural adjoint approach

Traditional Finite Differences Approach

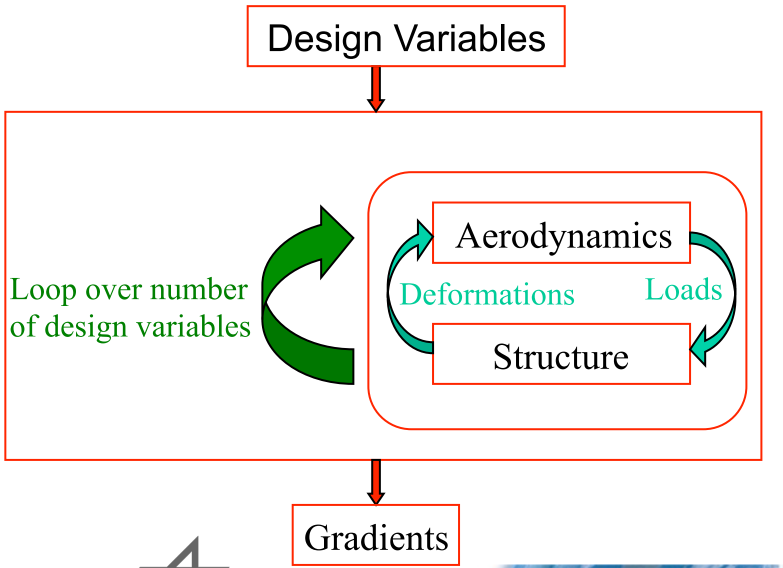

Coupled Adjoint Approach

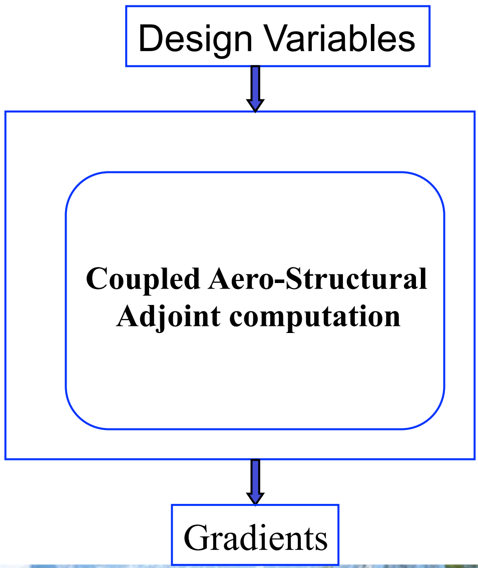

Adjoint approach
is independent on the
number of design variables

Formulation of the Coupled Adjoint Approach

Components of the Coupled System

- Loose aero-structural coupling is employed at DLR

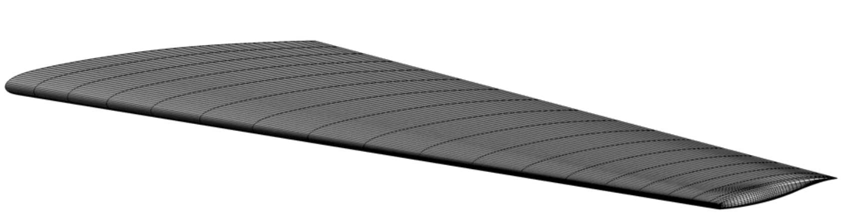

TAU

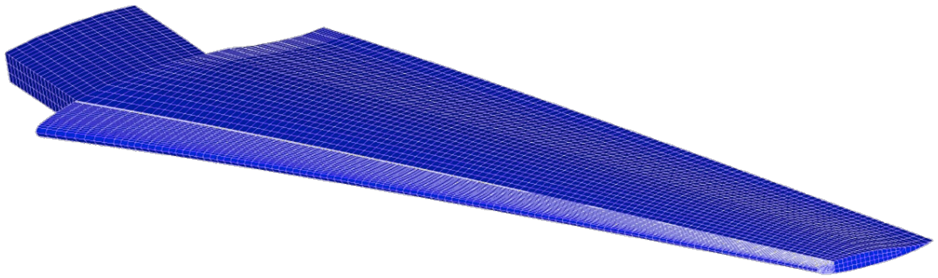

ANSYS

Components of the Coupled System

- Loose aero-structural coupling is employed at DLR

TAU

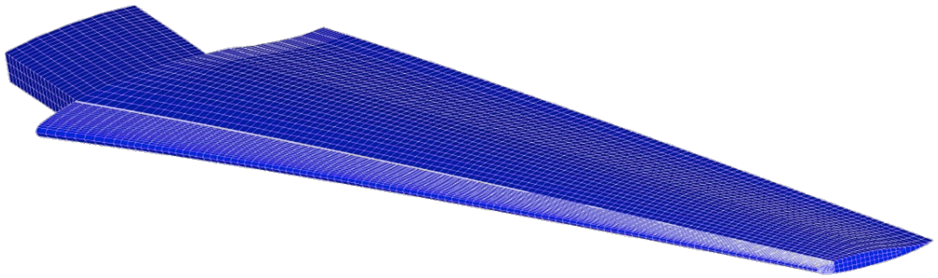

ANSYS

Components of the Coupled System

- Loose aero-structural coupling is employed at DLR

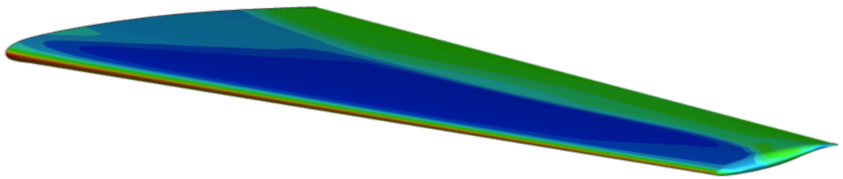

TAU

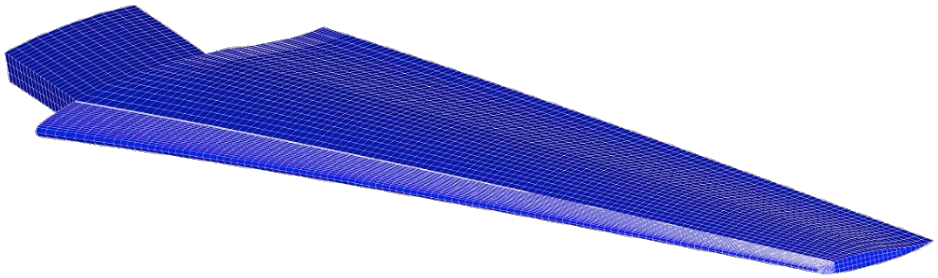

ANSYS

Components of the Coupled System

- Loose aero-structural coupling is employed at DLR

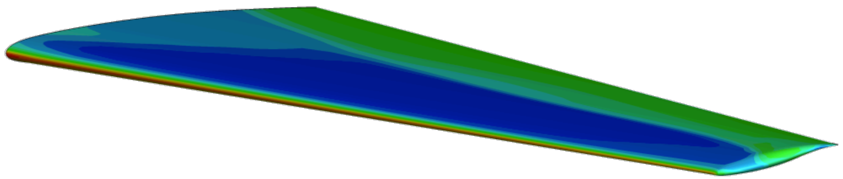

TAU

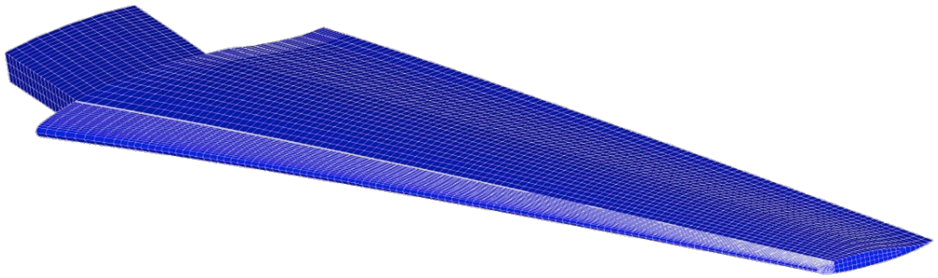

ANSYS

transfer loads from CFD mesh to CSM mesh using :
Linear Interpolation Tool

DLR

Components of the Coupled System

- Loose aero-structural coupling is employed at DLR

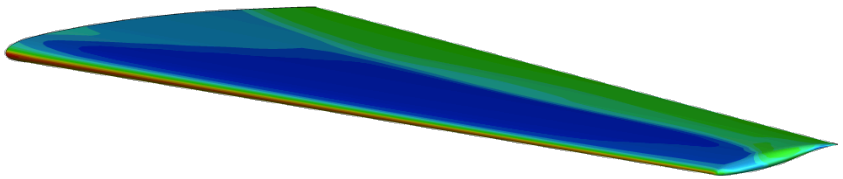

TAU

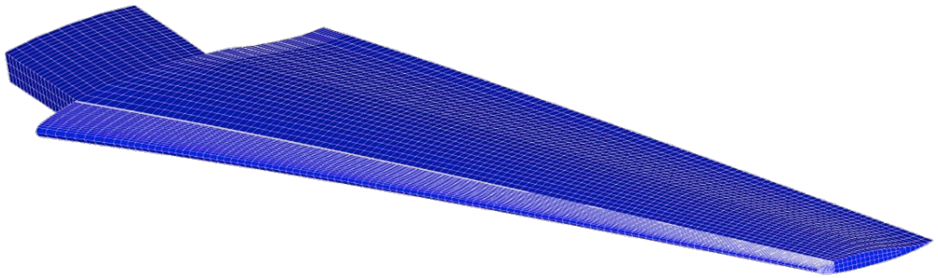

ANSYS

transfer loads from CFD mesh to CSM mesh using :
Linear Interpolation Tool

Components of the Coupled System

- Loose aero-structural coupling is employed at DLR

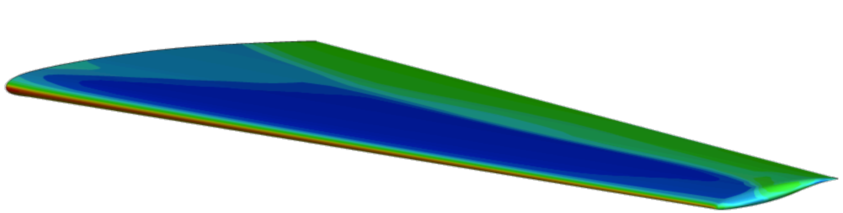

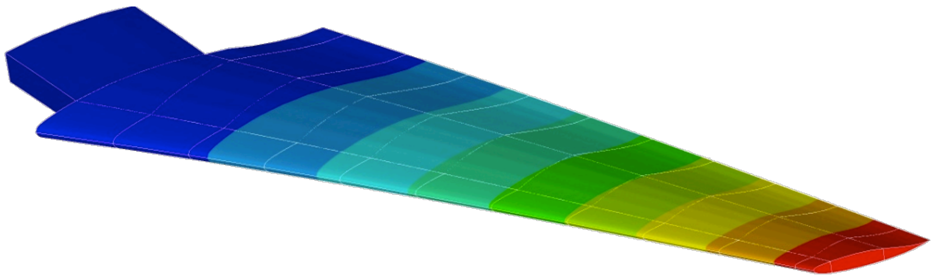

TAU

ANSYS

transfer loads from CFD mesh to CSM mesh using :
Linear Interpolation Tool

Components of the Coupled System

- Loose aero-structural coupling is employed at DLR

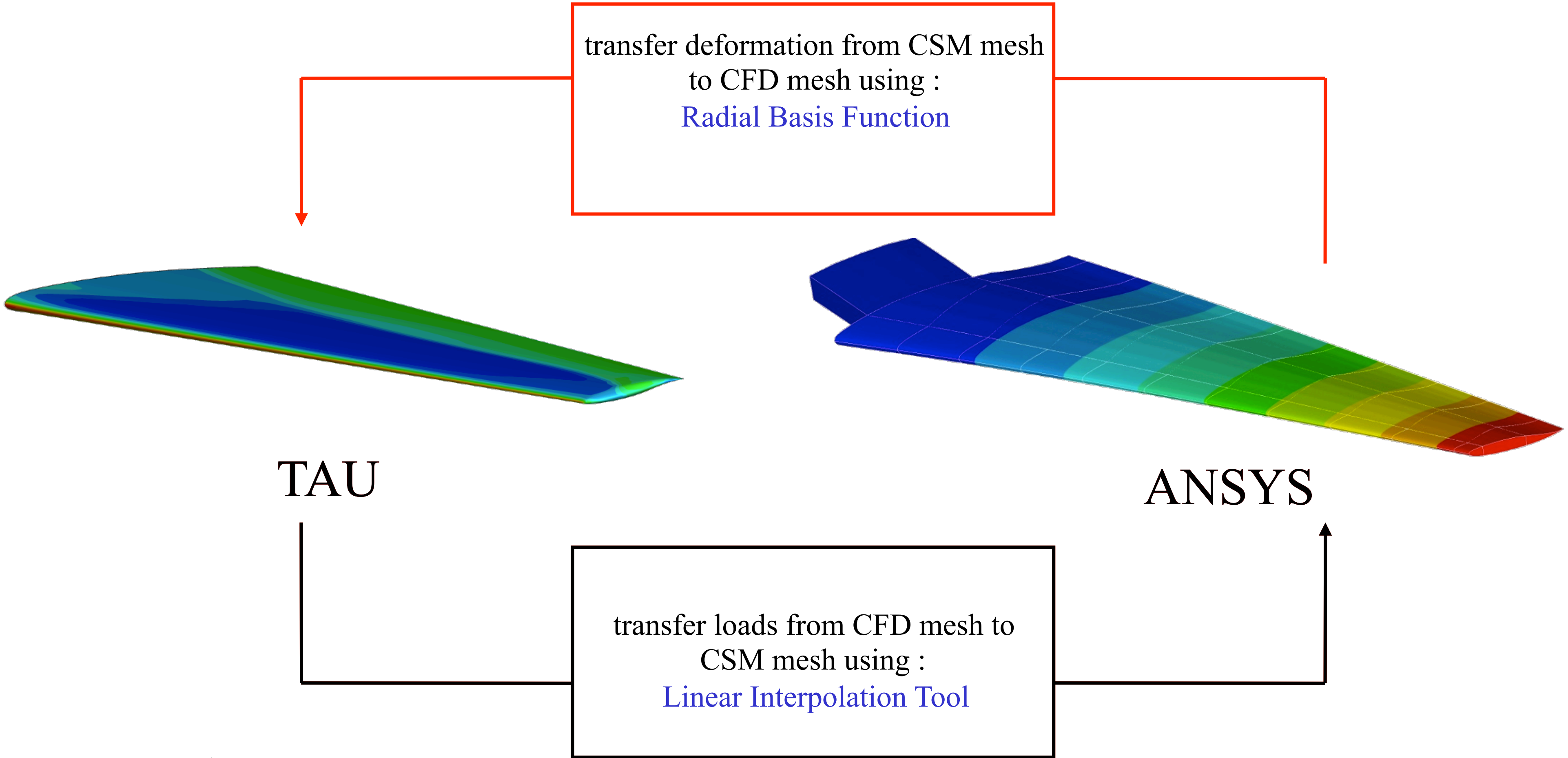

Components of the Coupled System

- Loose aero-structural coupling is employed at DLR

transfer deformation from CSM mesh to CFD mesh using :
Radial Basis Function

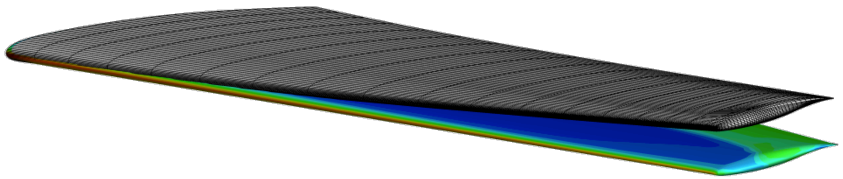

TAU

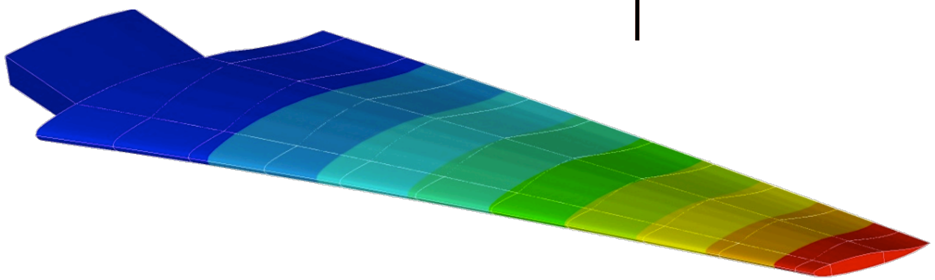

ANSYS

transfer loads from CFD mesh to CSM mesh using :
Linear Interpolation Tool

Components of the Coupled System

- Loose aero-structural coupling is employed at DLR

5 Couplings

transfer deformation from CSM mesh to CFD mesh using :
Radial Basis Function

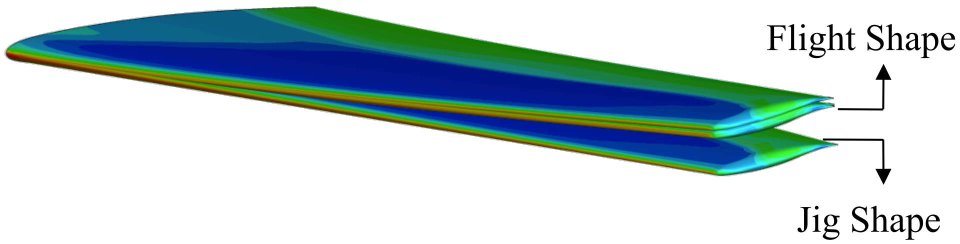

TAU

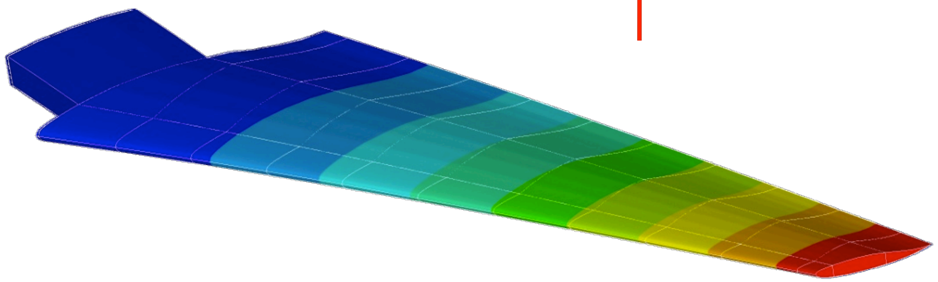

ANSYS

transfer loads from CFD mesh to CSM mesh using :
Linear Interpolation Tool

Formulation of the Coupled Adjoint Equations

- Motivation: Efficient computation of the gradient of a cost function (I) w.r.t the design parameters (D).
- The aero-structural coupled system is defined by:

I=I (W,D) ; R=R (W,D)=0

- Define the Lagrange: $L = I + \Psi R$

Residual Vector	$R = \begin{bmatrix} Ra \\ Rs \end{bmatrix}$	Aerodynamic residual Structural residual
State variables Vector	$W = \begin{bmatrix} w \\ u \end{bmatrix}$	Flow variables Structural deformation
Design variables Vector	$D = \begin{bmatrix} A \\ T \end{bmatrix}$	Shape design variables Structural thickness

$$\begin{bmatrix} \frac{\partial \mathbf{Ra}}{\partial \mathbf{w}}^T & \frac{\partial \mathbf{Ra}}{\partial \mathbf{u}}^T \\ \frac{\partial \mathbf{Rs}}{\partial \mathbf{w}}^T & \frac{\partial \mathbf{Rs}}{\partial \mathbf{u}}^T \end{bmatrix} \begin{Bmatrix} \psi \mathbf{a} \\ \psi \mathbf{s} \end{Bmatrix} = - \begin{bmatrix} \frac{\partial I}{\partial \mathbf{w}} \\ \frac{\partial I}{\partial \mathbf{u}} \end{bmatrix}$$

The Coupled Adjoint Equation

$$\begin{Bmatrix} \frac{dI}{d\mathbf{D}} \end{Bmatrix}^T = \begin{Bmatrix} \frac{dL}{d\mathbf{D}} \end{Bmatrix}^T = \left(\begin{Bmatrix} \frac{\partial I}{\partial \mathbf{A}} \\ \frac{\partial I}{\partial \mathbf{T}} \end{Bmatrix}^T + \begin{Bmatrix} \psi \mathbf{a} \\ \psi \mathbf{s} \end{Bmatrix}^T \begin{bmatrix} \frac{\partial \mathbf{Ra}}{\partial \mathbf{A}} & \frac{\partial \mathbf{Ra}}{\partial \mathbf{T}} \\ \frac{\partial \mathbf{Rs}}{\partial \mathbf{A}} & \frac{\partial \mathbf{Rs}}{\partial \mathbf{T}} \end{bmatrix} \right)$$

The Gradients

Where ψa and ψs are the aerodynamic and the structure Lagrange multipliers.

Test case description

DLR

Test Case Description

- Wing-Body configuration based on the DO728 geometry used as a test case.
- Reynolds number : 21e06
- Lift is kept constant by varying angle of attack (implicit lift constraint → requires gradient correction)

- CFD
- One-Equation turbulence model Spalart-Allmaras

Test Case Description

- Wing-Body configuration based on the DO728 geometry used as a test case.
- Reynolds number : 21e06
- Lift is kept constant by varying angle of attack (implicit lift constraint → requires gradient correction)

- CFD
- One-Equation turbulence model Spalart-Allmaras
- CFD structured mesh; 1.2 Million nodes
- .
- .
- .

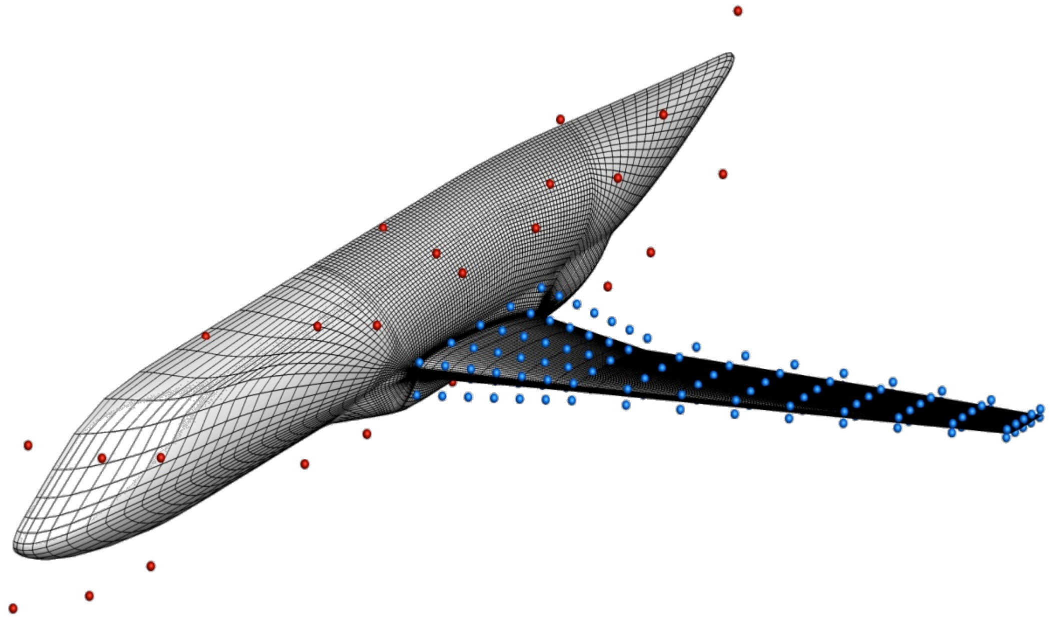

Test Case Description

- Wing-Body configuration based on the DO728 geometry used as a test case.
- Reynolds number : 21e06
- Lift is kept constant by varying angle of attack (implicit lift constraint → requires gradient correction)

- CFD
- One-Equation turbulence model Spalart-Allmaras
- CFD structured mesh; 1.2 Million nodes
- Parameterization: 30 parameters fixing the body
  150/2 FFD parameters on the wing
  (implicit thickness constraint)

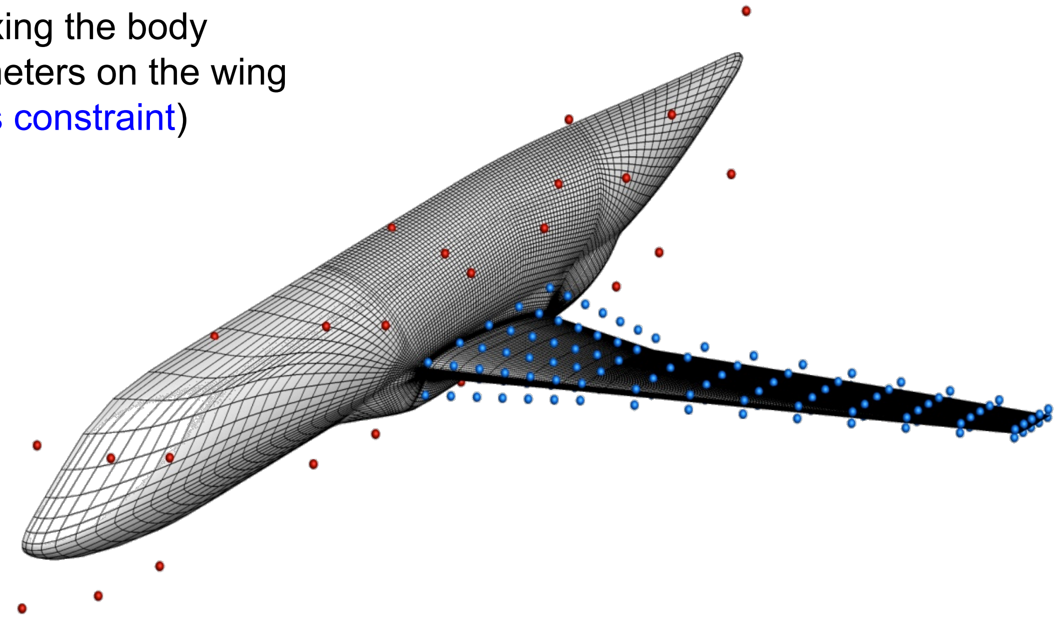

Test Case Description

- Wing-Body configuration based on the DO728 geometry used as a test case.
- Reynolds number : 21e06
- Lift is kept constant by varying angle of attack (implicit lift constraint → requires gradient correction)

$$\frac{d(C_D)@\text{constant Lift}}{dA} = \frac{dC_D}{dA} - \left(\frac{dC_D}{d\alpha} / \frac{dC_L}{d\alpha}\right)\frac{dC_L}{dA}$$

- CFD
- One-Equation turbulence model Spalart-Allmaras
- CFD structured mesh; 1.2 Million nodes
- Parameterization: 30 parameters fixing the body
  150/2 FFD parameters on the wing
  (implicit thickness constraint)

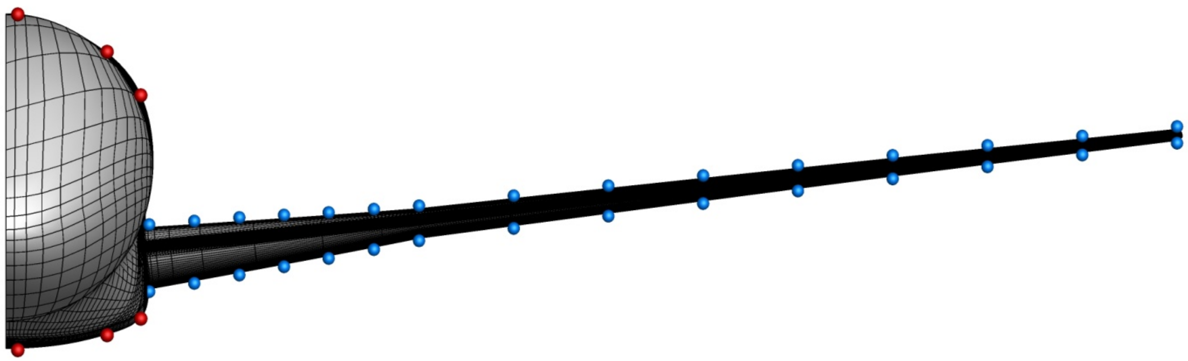

Test Case Description

- Wing-Body configuration based on the DO728 geometry used as a test case.
- The Structure model:
  - 27 Ribs
  - 2 Spars
  - Lower & Upper Skin

.
.
.
.

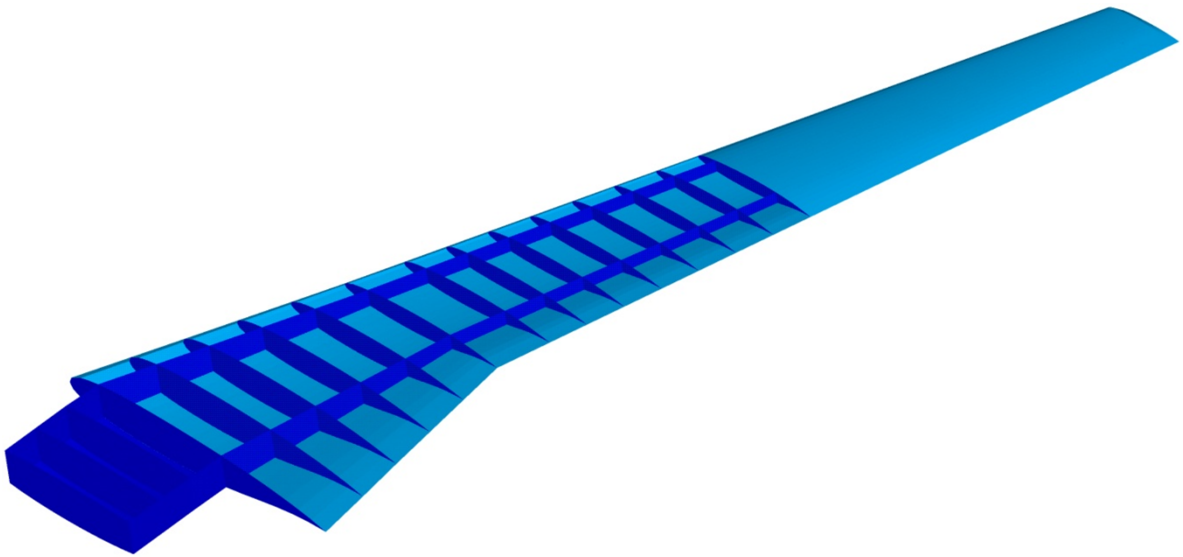

Test Case Description

- Wing-Body configuration based on the DO728 geometry used as a test case.
- The Structure model:
  27 Ribs
  2 Spars
  Lower & Upper Skin
- CSM
- The CSM mesh:
  4000 nodes.
  Modeled using rectangular shell elements,
  each node has 6 DOFs.

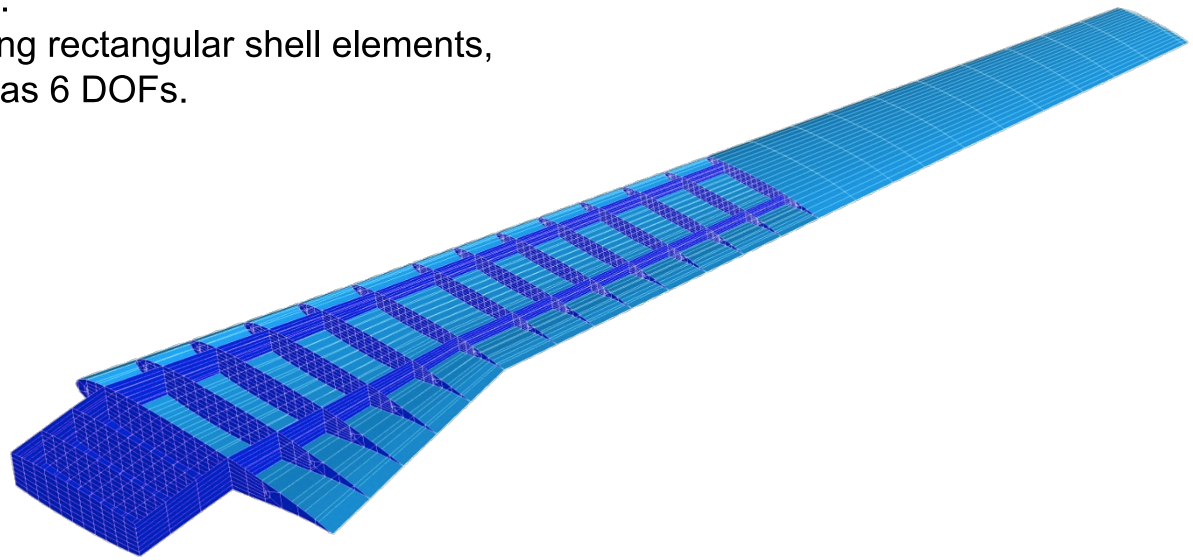

Optimizations

DLR

Optimizations

- Three optimizations were performed

Optimizations

- Three optimizations were performed

- 1. Unconstrained Single-point optimization
  at the design point
- .
- .

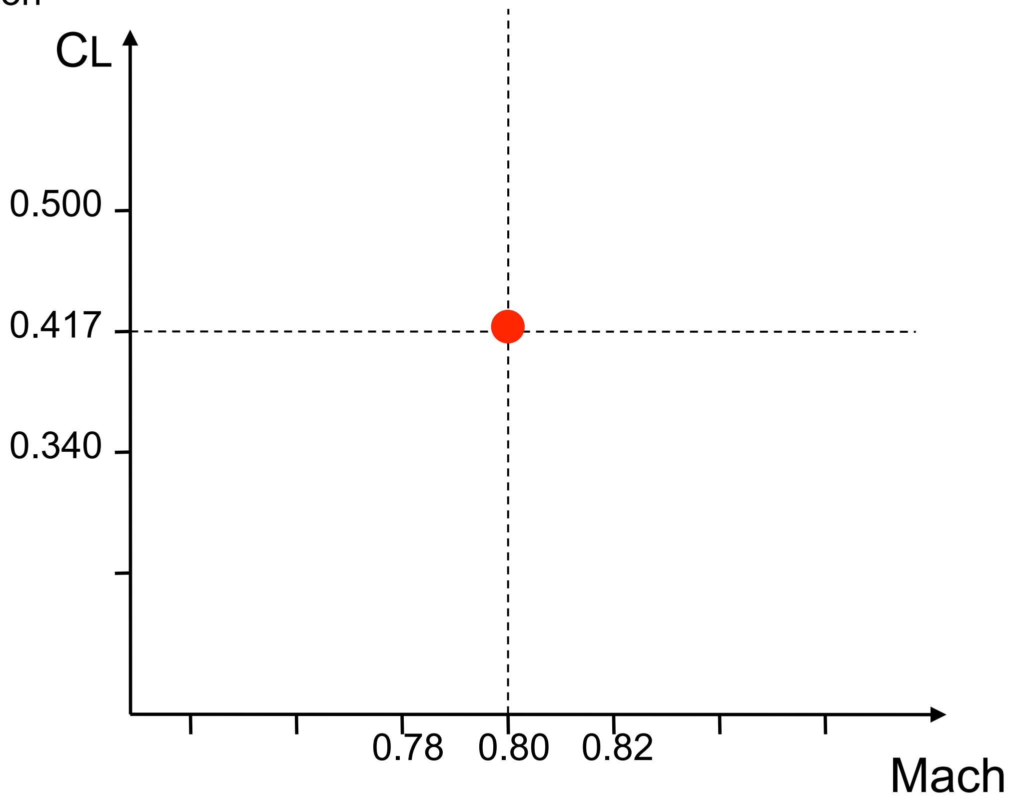

Optimizations

- Three optimizations were performed

- 1. Unconstrained Single-point optimization at the design point
- 2. Constrained Single-point optimization at the design point

.

.

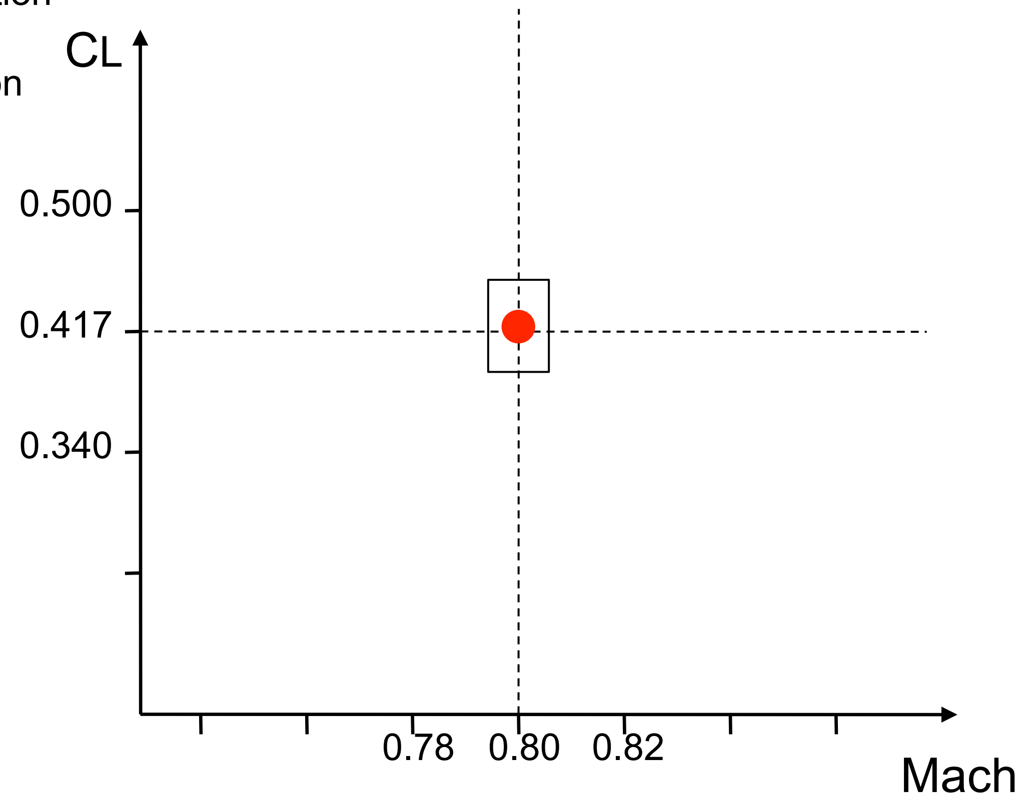

Optimizations

- Three optimizations were performed

- 1. Unconstrained Single-point optimization at the design point
- 2. Constrained Single-point optimization at the design point
- 3. Constrained Multi-Point Optimization

.

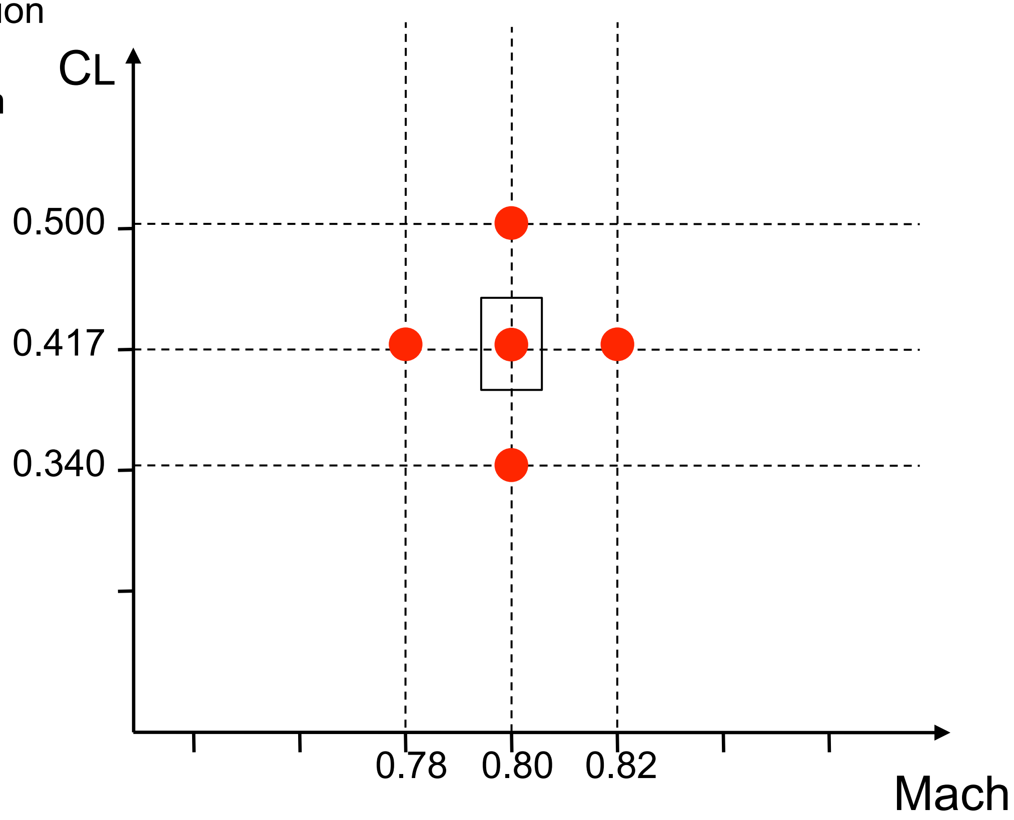

Optimizations

- Three optimizations were performed

- 1. Unconstrained Single-point optimization at the design point
- 2. Constrained Single-point optimization at the design point
- 3. Constrained Multi-Point Optimization

- The objective is drag reduction at constant CL and wing thickness. (Aerodynamic objective with elastic effects taken into account)

.

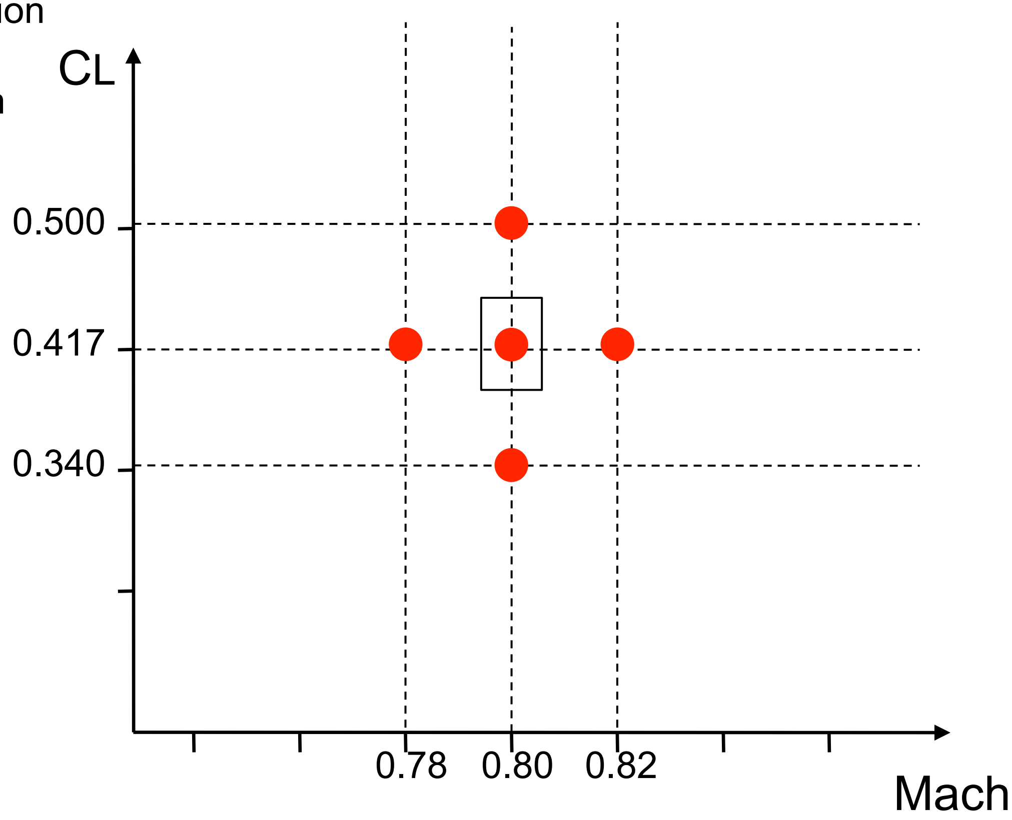

Unconstrained Single-point Optimization

- The optimization employed a quasi-Newton gradient-based algorithm.
-
-

Unconstrained Single-point Optimization

- The optimization employed a quasi-Newton gradient-based algorithm.
- Optimization converged after 41 aero-structural couplings and 25 coupled adjoint computations.
- The optimization reduced the drag by 15 drag counts while keeping the lift and the thickness constant.

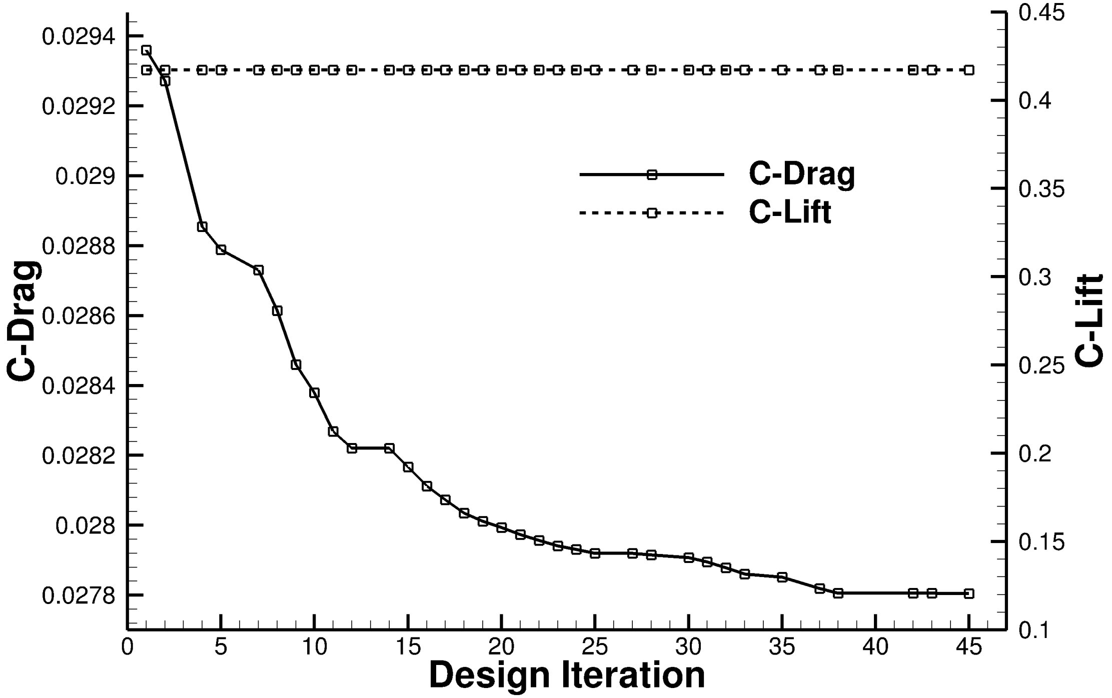

Unconstrained Single-point Optimization

- The optimization employed a quasi-Newton gradient-based algorithm.
- Optimization converged after 41 aero-structural couplings and 25 coupled adjoint computations.
- The optimization reduced the drag by 15 drag counts while keeping the lift and the thickness constant.

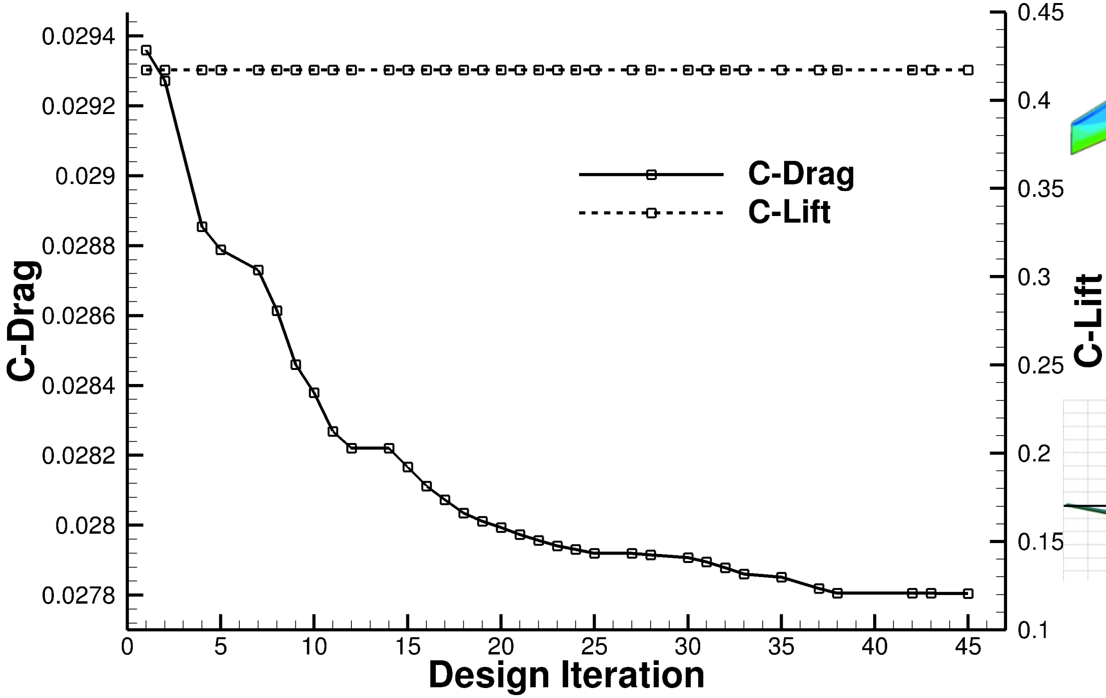

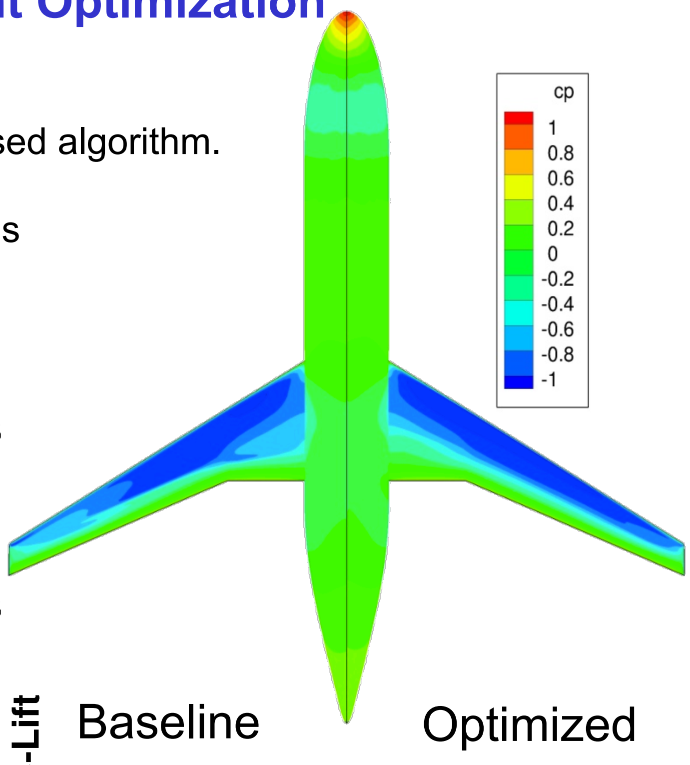

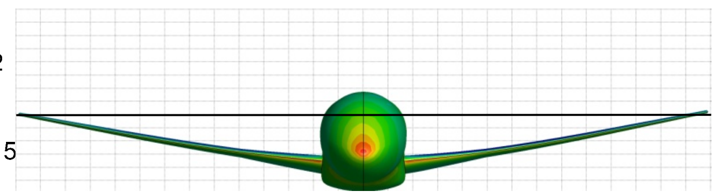

Unconstrained Single-point Optimization

- The optimization employed a quasi-Newton gradient-based algorithm.
- Optimization converged after 41 aero-structural couplings and 25 coupled adjoint computations.
- The optimization reduced the drag by 15 drag counts while keeping the lift and the thickness constant.

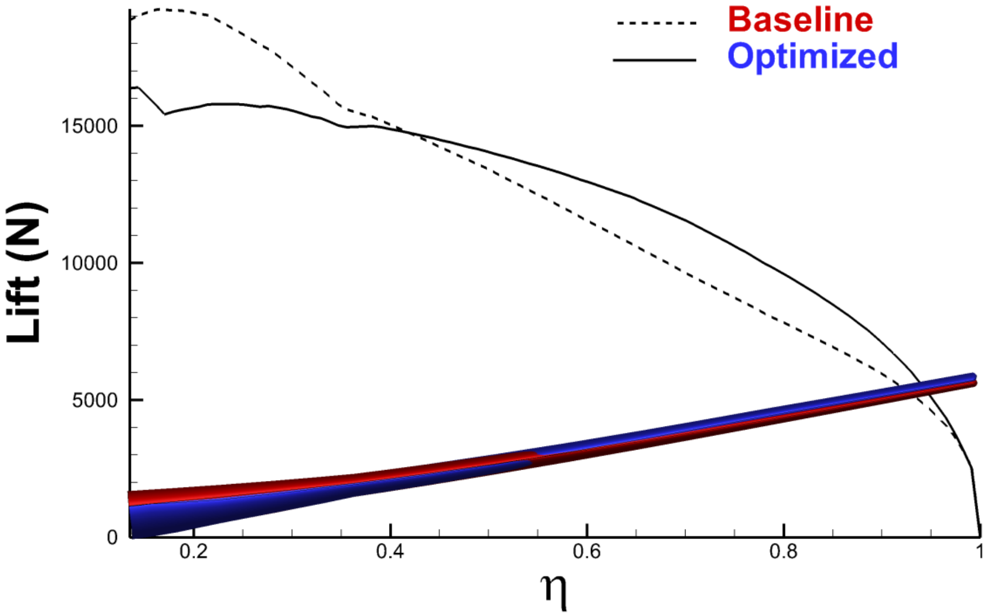

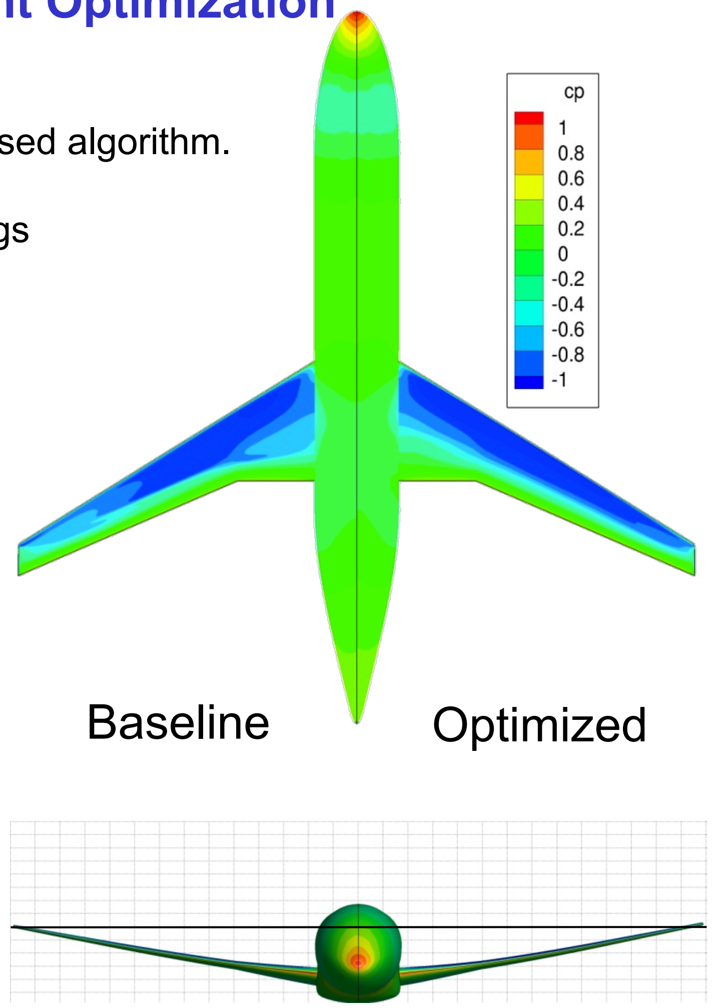

Unconstrained Single-point Optimization

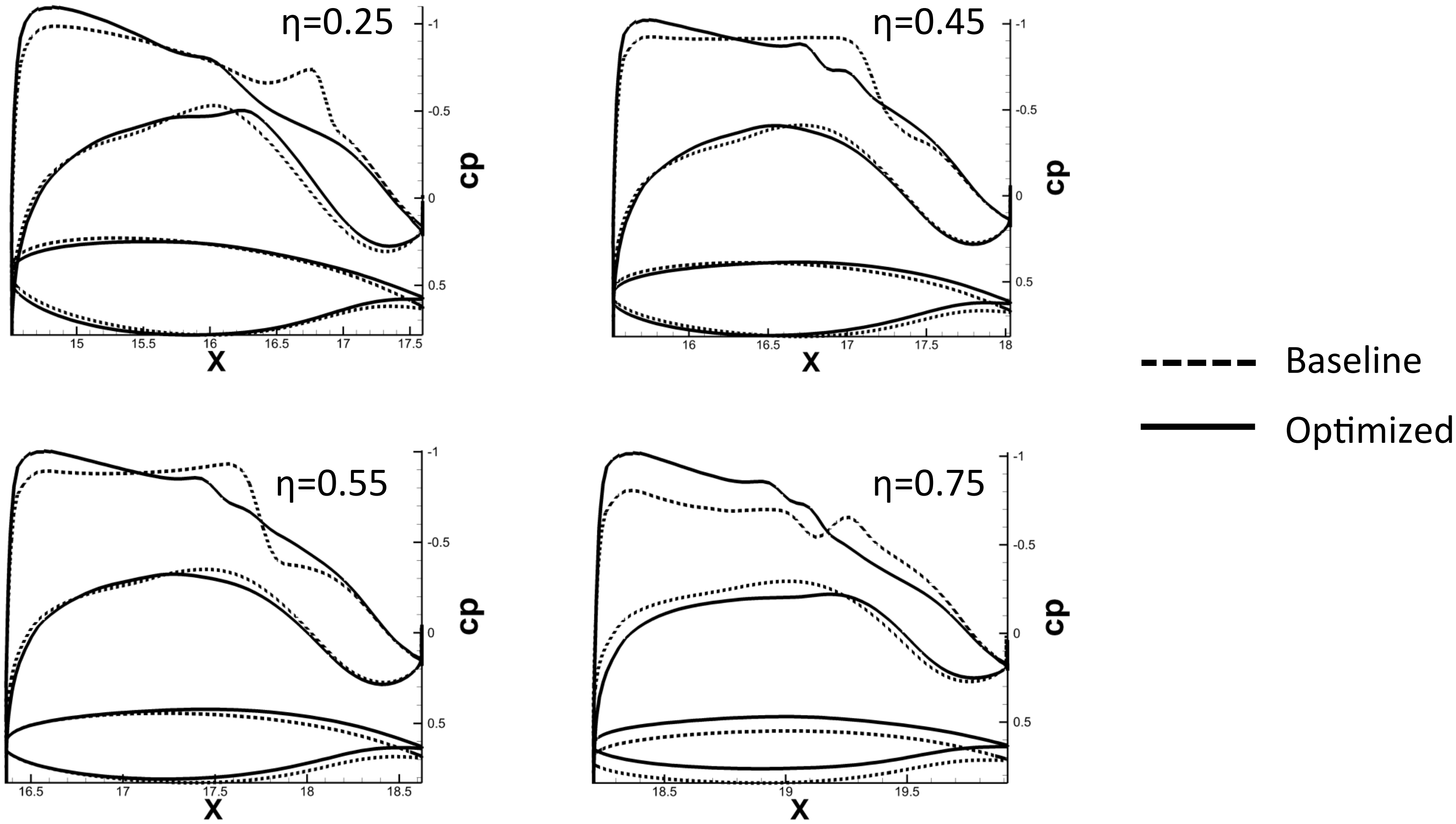

Unconstrained Single-point Optimization

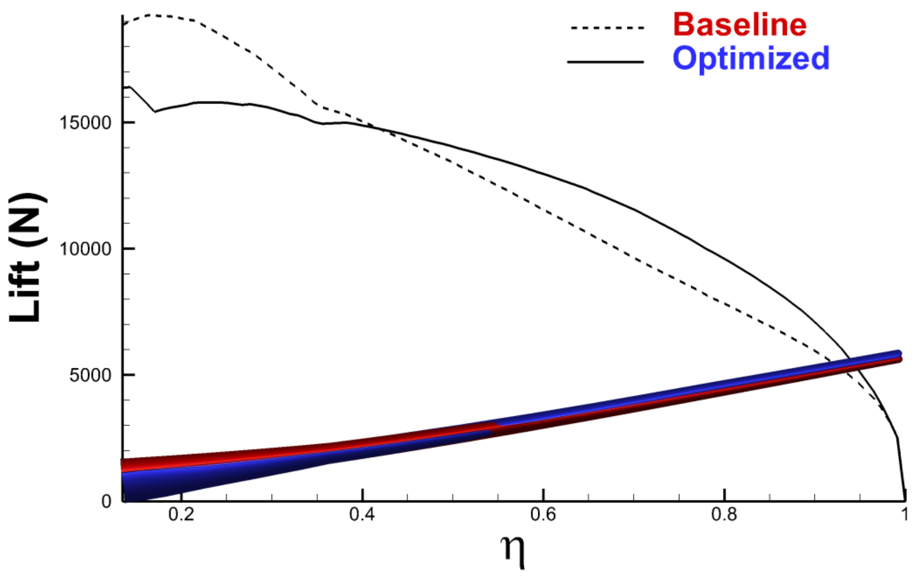

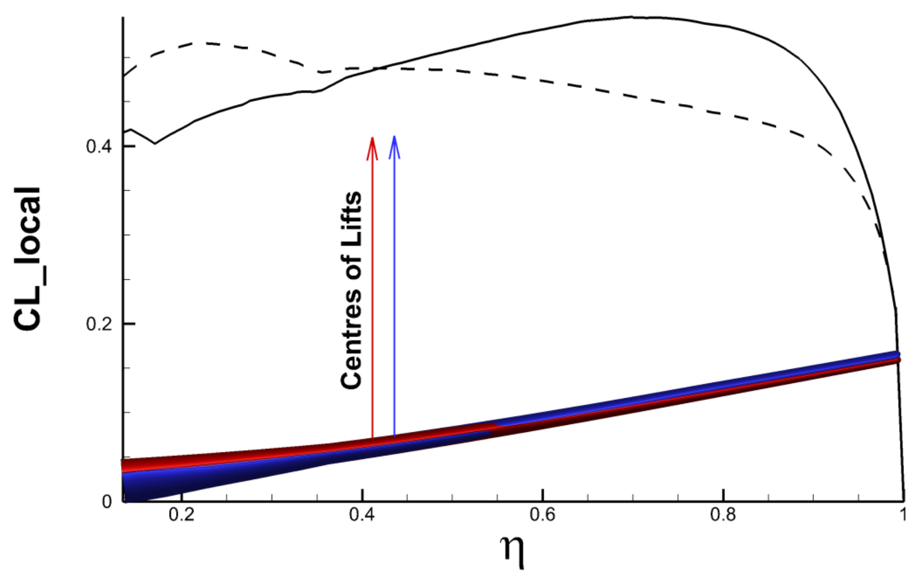

Unconstrained Single-point Optimization

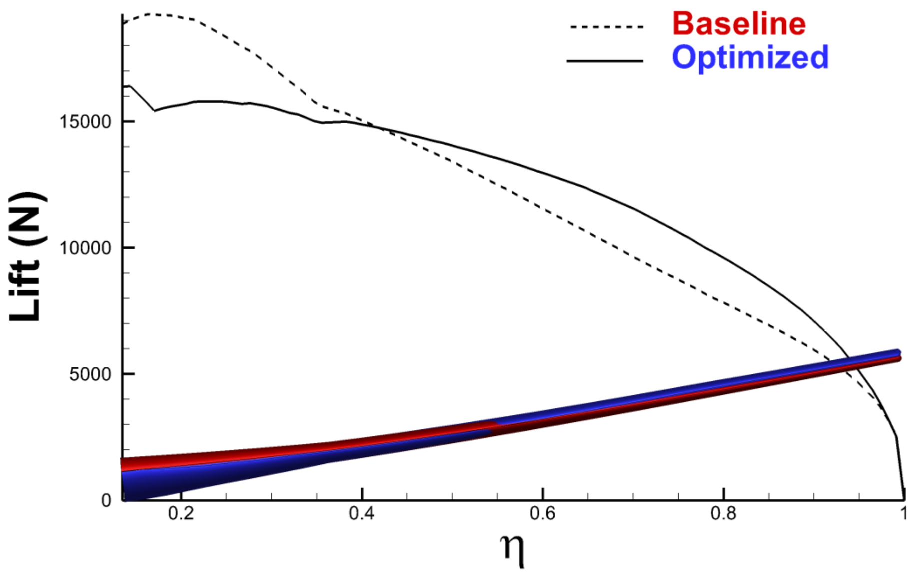

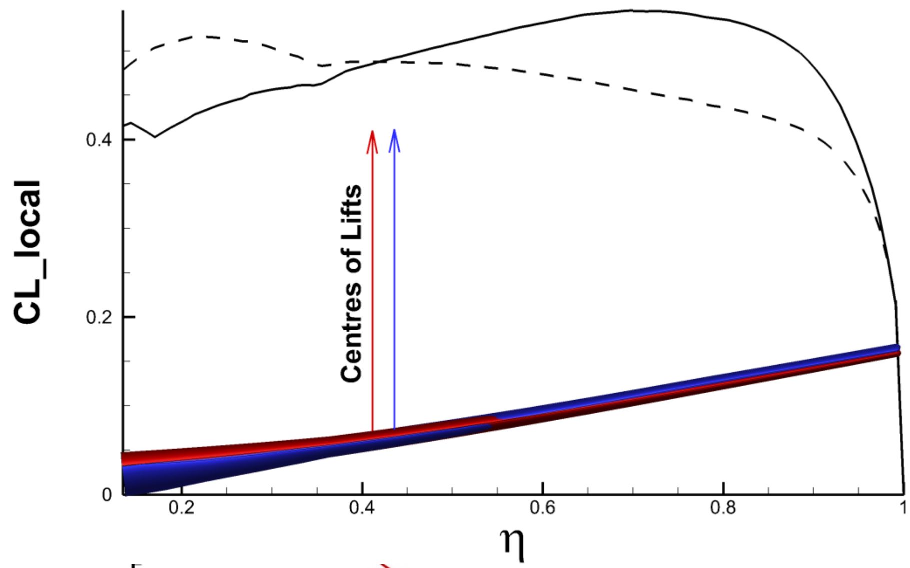

This (at constant lift) increases the bending moment at the Wing's root

⇒ Keep CMx constant during the aero-elastic optimization

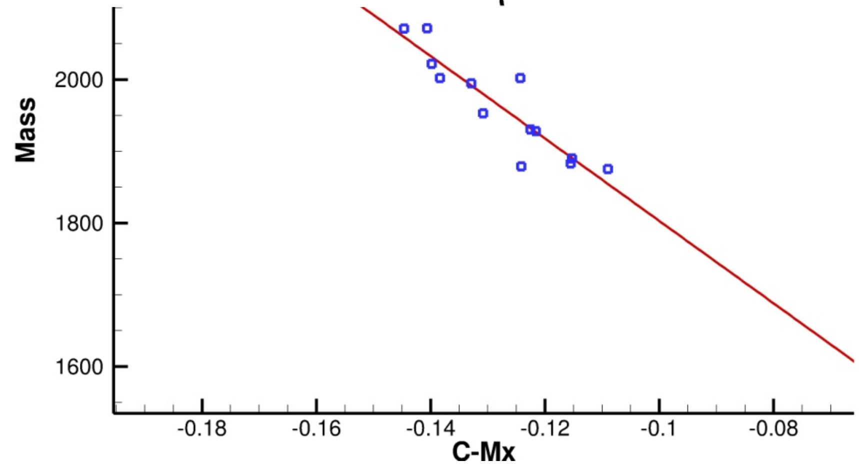

DLR

Constrained Single-point Optimization

- The optimization employed SQP gradient-based algorithm.
- Optimization converged after 31 aero-structural couplings and 19 coupled adjoint computations.
- The optimization reduced the drag by 13 drag counts while keeping the lift and the thickness constant.

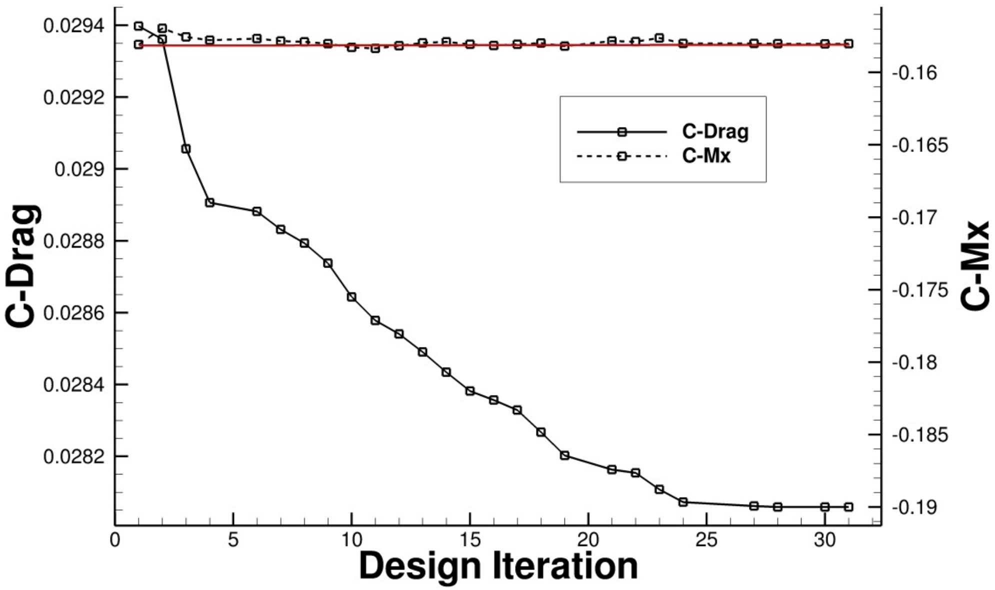

Constrained Single-point Optimization

- The optimization employed SQP gradient-based algorithm.
- Optimization converged after 31 aero-structural couplings and 19 coupled adjoint computations.
- The optimization reduced the drag by 13 drag counts while keeping the lift and the thickness constant.

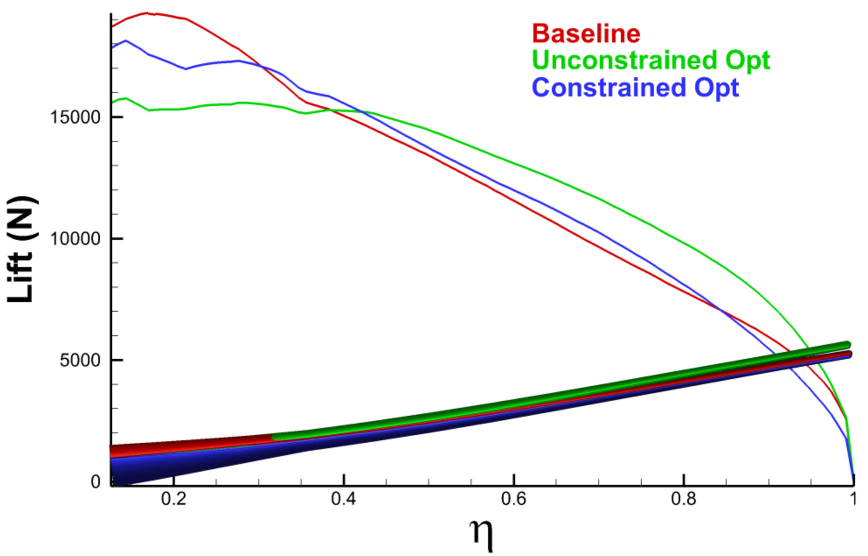

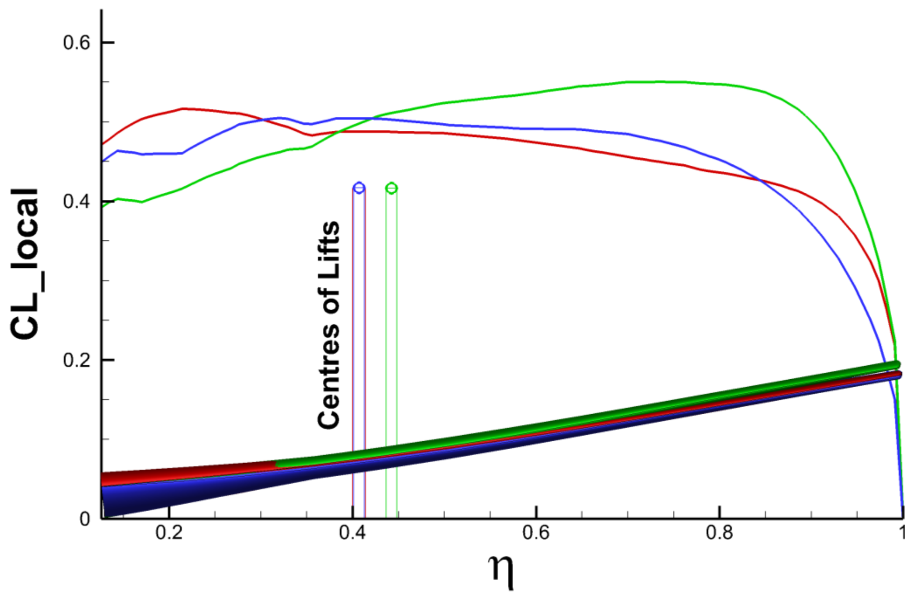

Constrained Single-point Optimization

- The optimization employed SQP gradient-based algorithm.

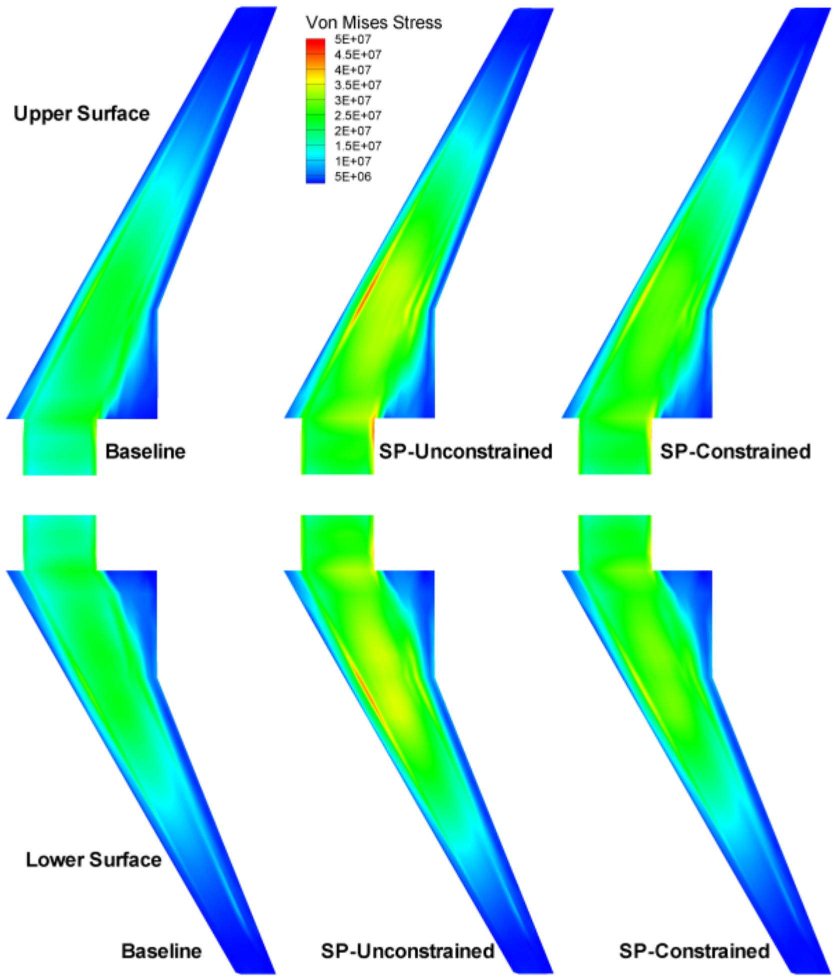

Constrained Multi-point Optimization

- The points were equally weighted.

$$\text{Cost\_Function} = \sum_{i=1}^{5} 0.2 * C_{Di}$$

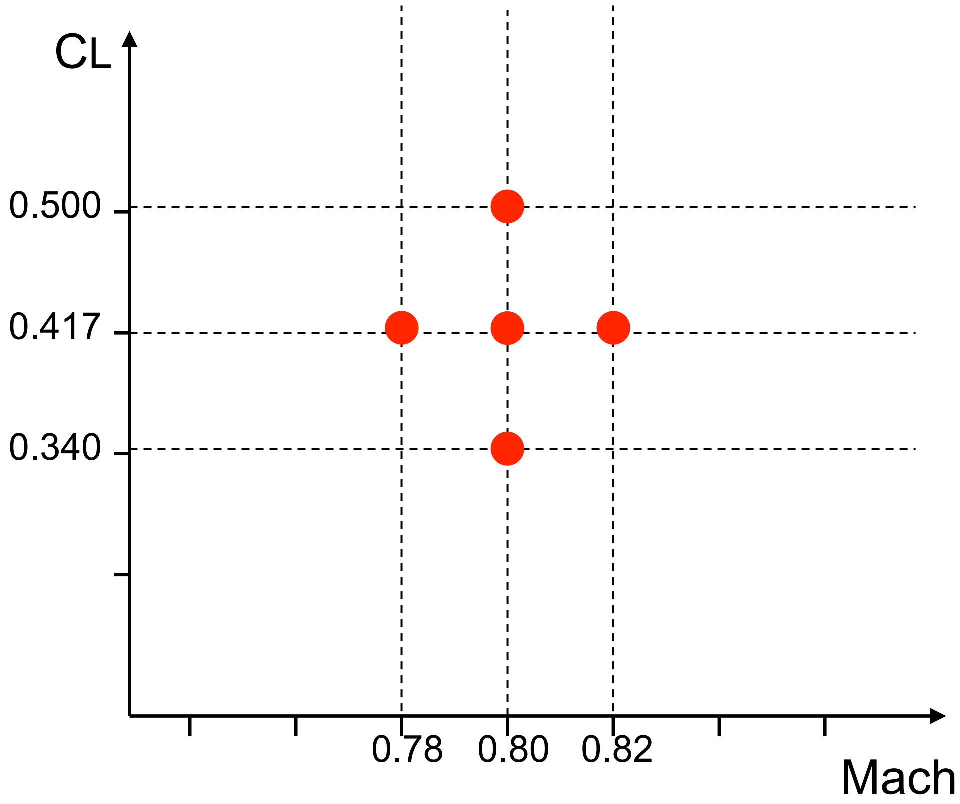

Constrained Multi-point Optimization

- The points were equally weighted.

$$\text{Cost\_Function} = \sum_{i=1}^{5} 0.2 * C_{Di}$$

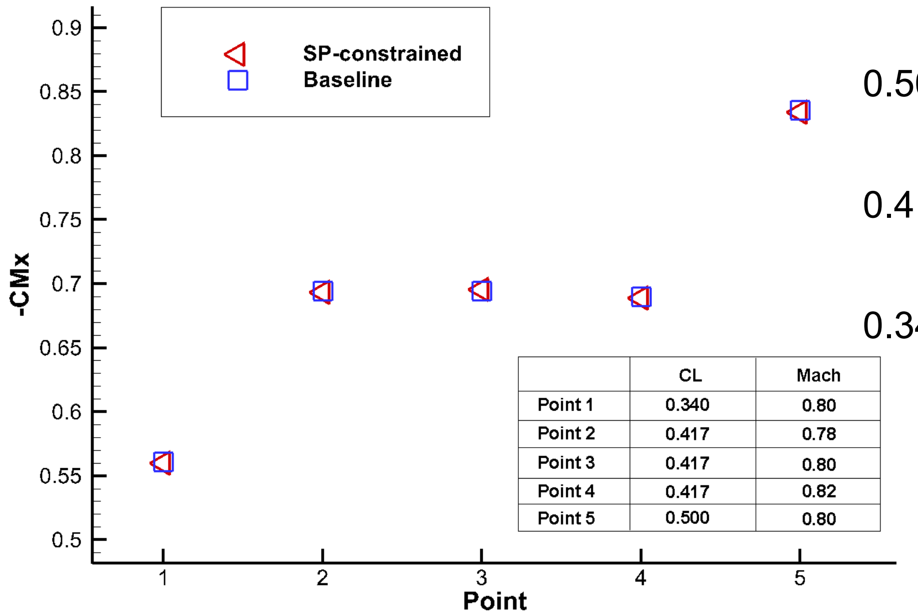

	CL	Mach
Point 1	0.340	0.80
Point 2	0.417	0.78
Point 3	0.417	0.80
Point 4	0.417	0.82
Point 5	0.500	0.80

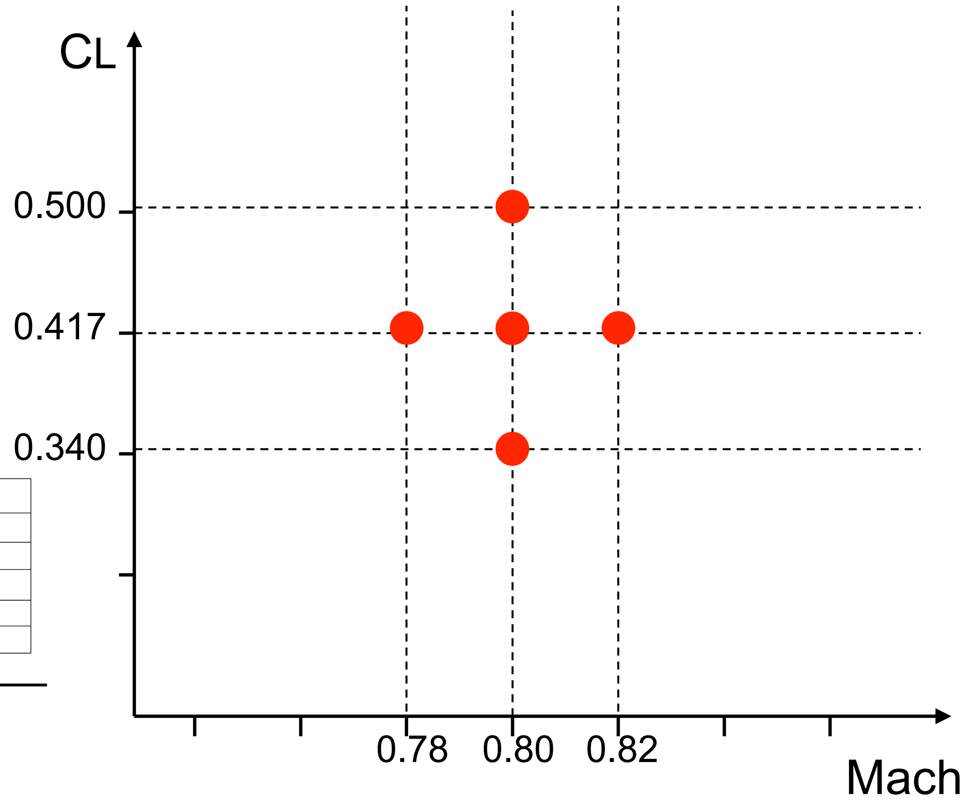

Constrained Multi-point Optimization

- The points were equally weighted.

$$\text{Cost\_Function} = \sum_{i=1}^{5} 0.2 * C_{Di}$$

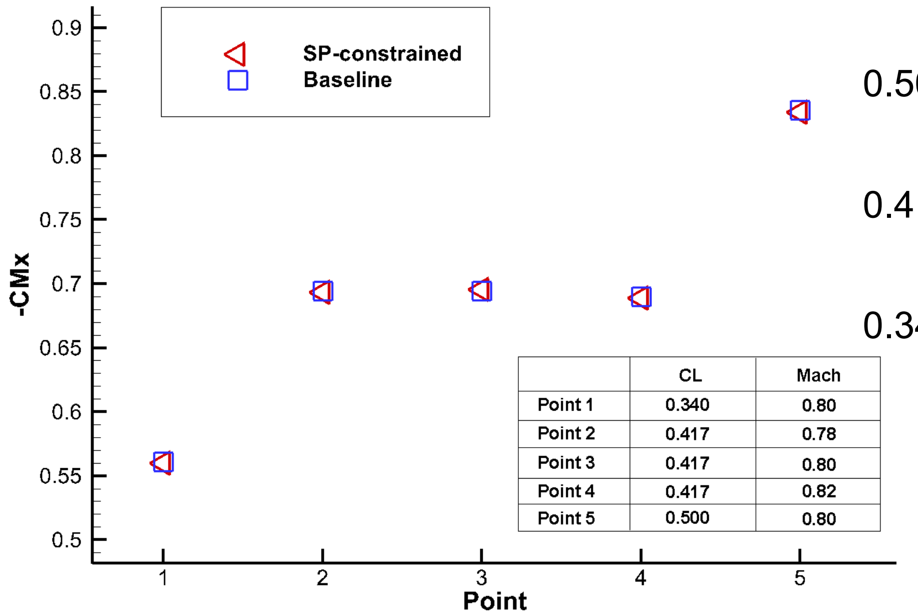

	CL	Mach
Point 1	0.340	0.80
Point 2	0.417	0.78
Point 3	0.417	0.80
Point 4	0.417	0.82
Point 5	0.500	0.80

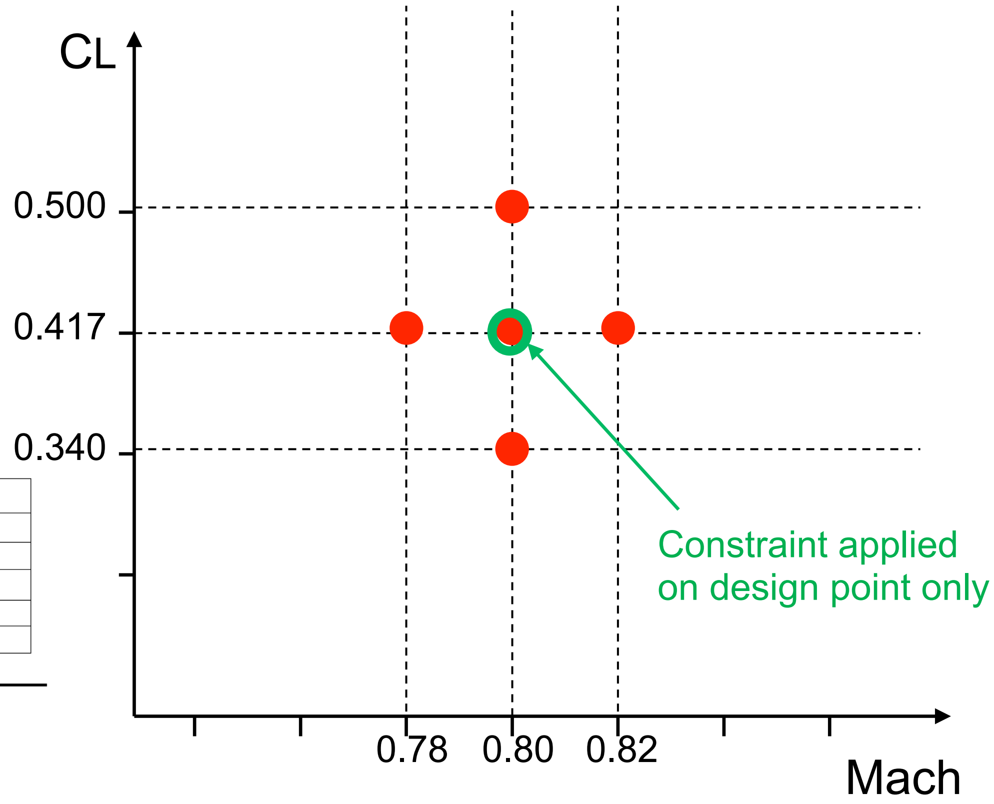

DLR

Constrained Multi-point Optimization

- The points were equally weighted. → Highest gradients bring highest change (drag reduction)

$$\text{Cost\_Function} = \sum_{i=1}^{5} 0.2 * C_{Di}$$

- 25 design iterations
- 20 gradient computations
- 260 hrs on 48 processors

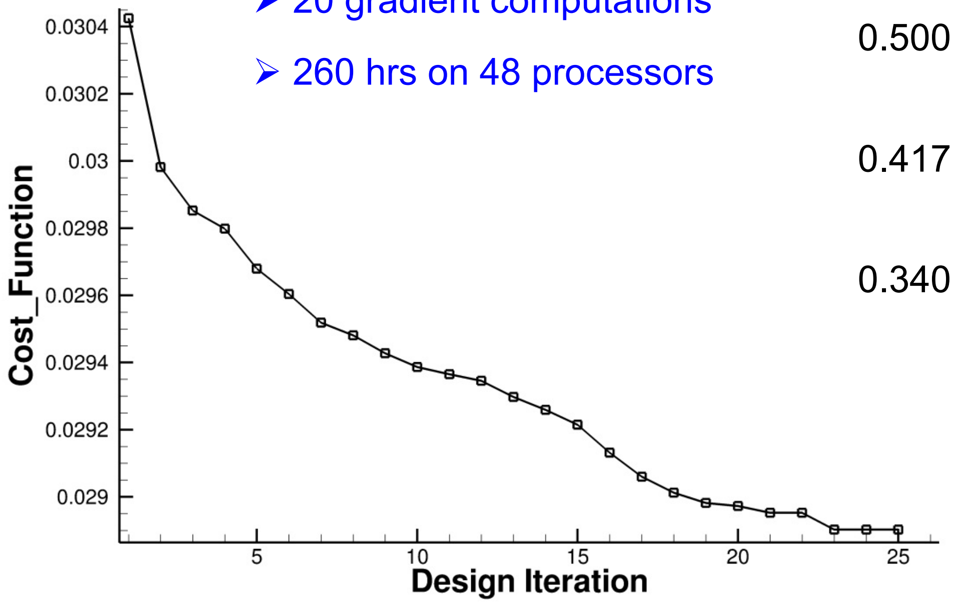

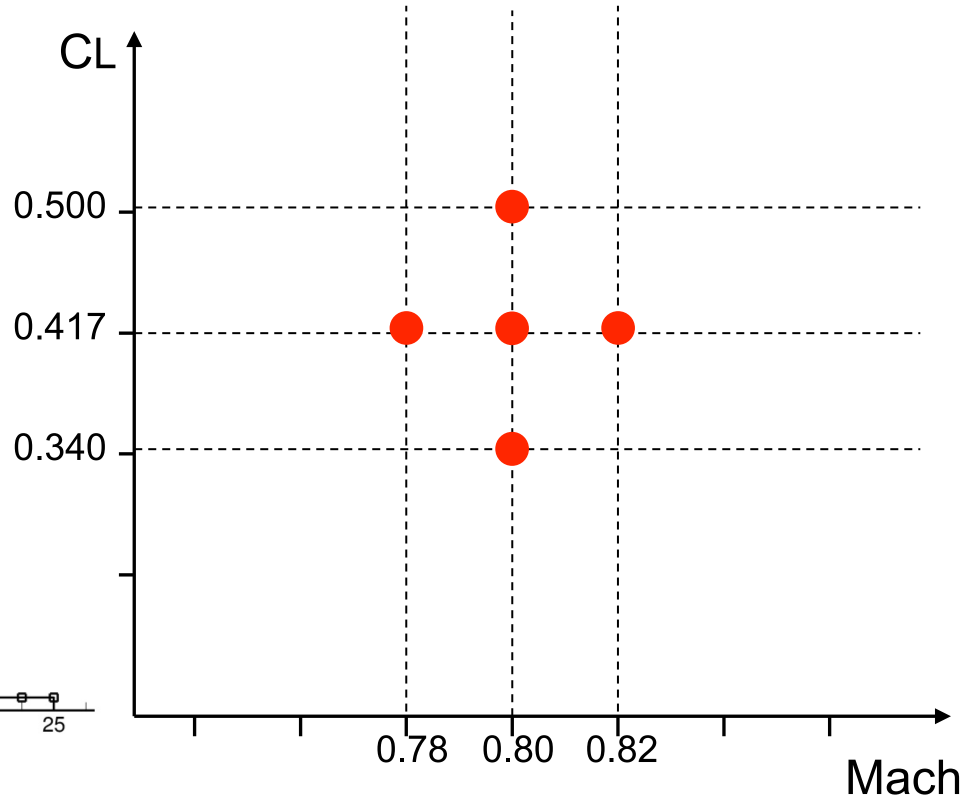

Constrained Multi-point Optimization

- The points were equally weighted. → Highest gradients bring highest change (drag reduction)

$$\text{Cost\_Function} = \sum_{i=1}^{5} 0.2 * C_{Di}$$

- 25 design iterations
- 20 gradient computations
- 260 hrs on 48 processors

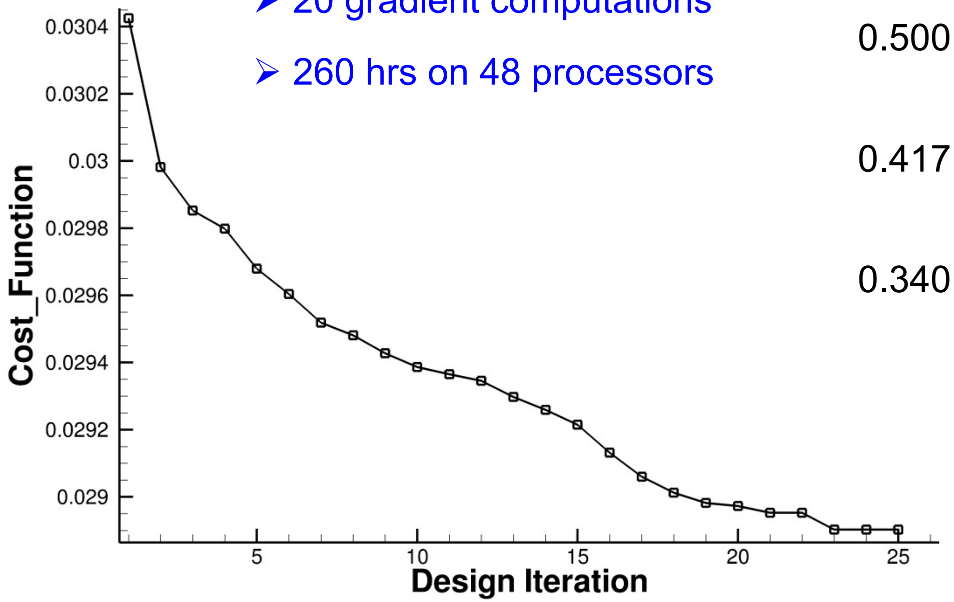

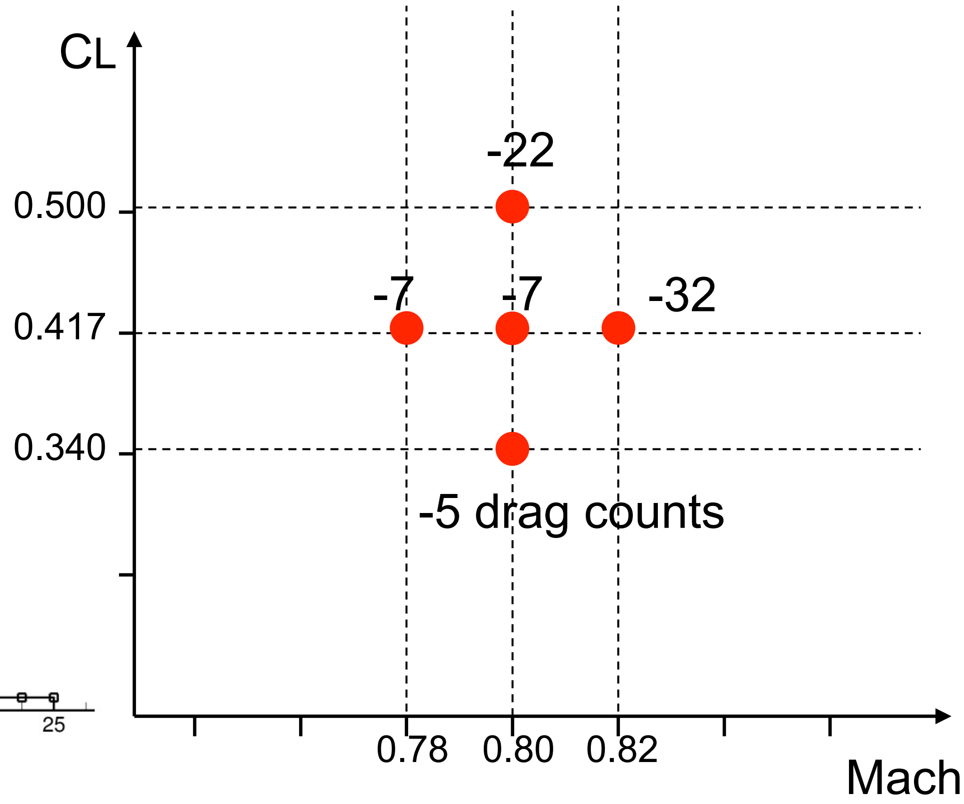

Constrained Multi-point Optimization

- The points were equally weighted. → Highest gradients bring highest change (drag reduction)

$$\text{Cost\_Function} = \sum_{i=1}^{5} 0.2 * C_{Di}$$

- 25 design iterations
- 20 gradient computations
- 260 hrs on 48 processors

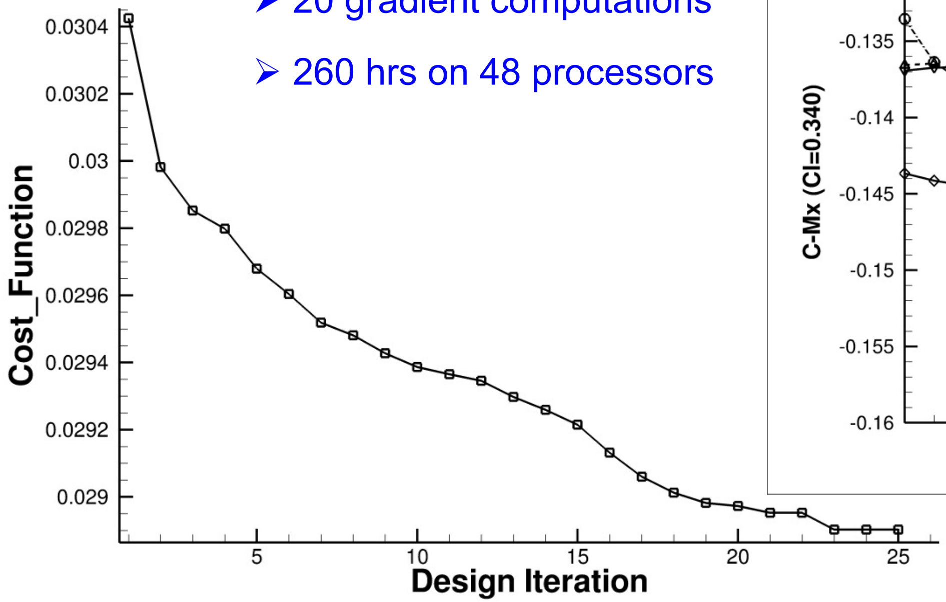

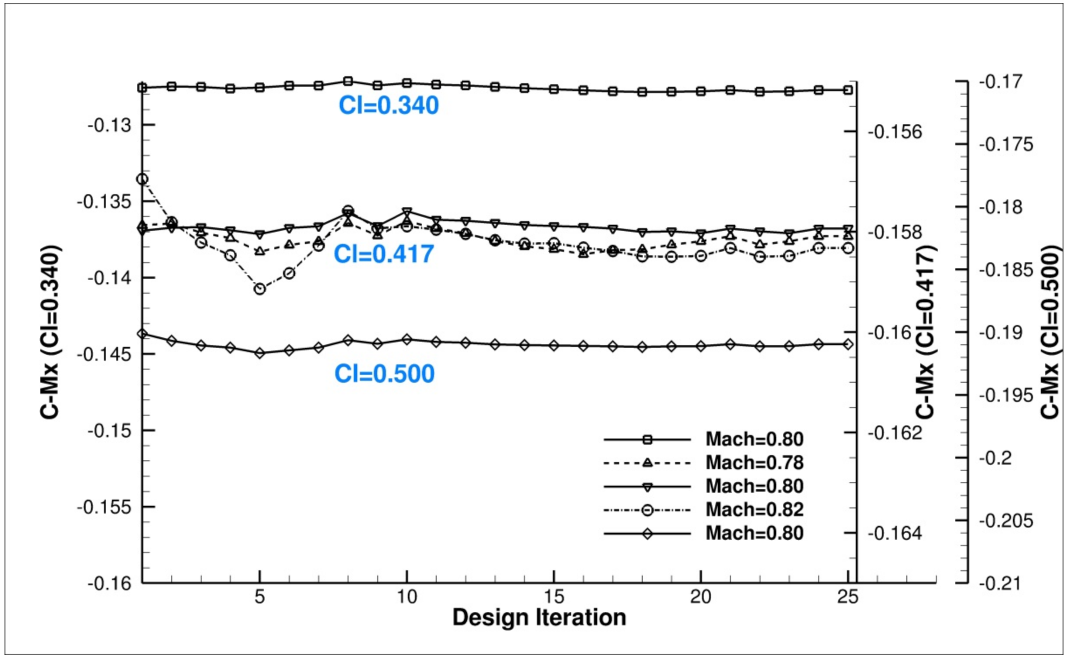

Constrained Multi-point Optimization

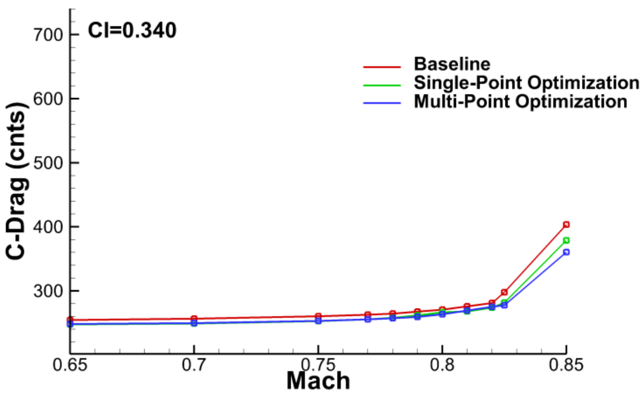

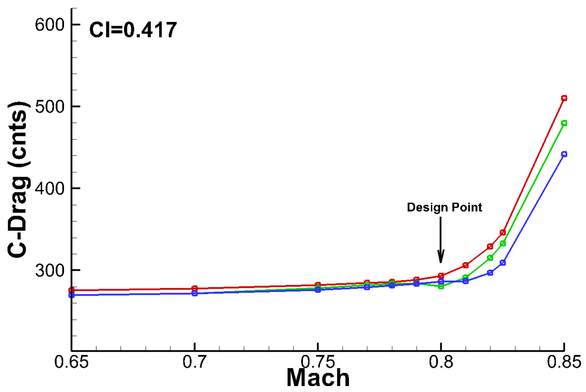

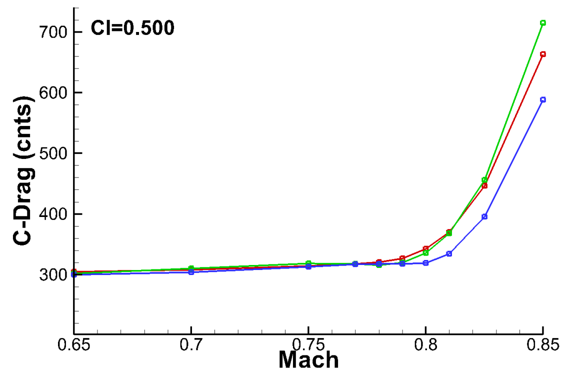

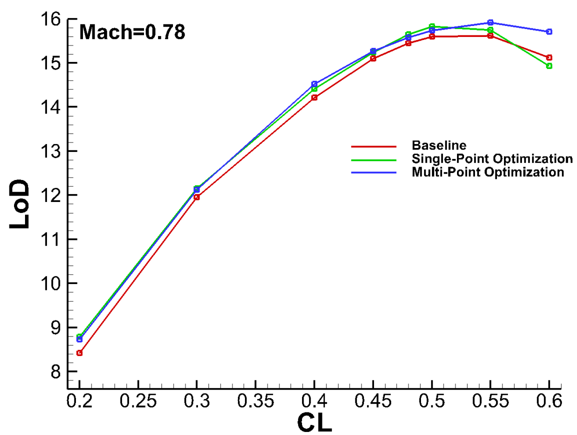

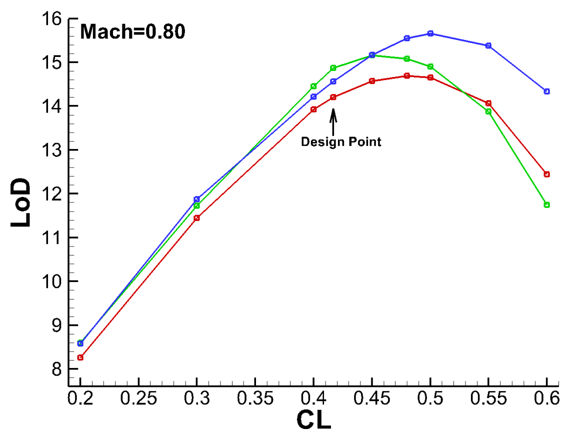

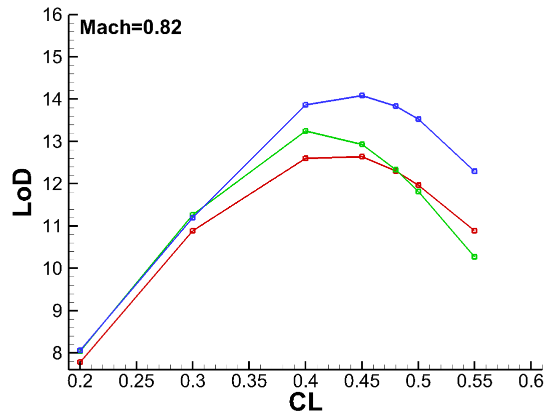

Constrained Multi-point Optimization

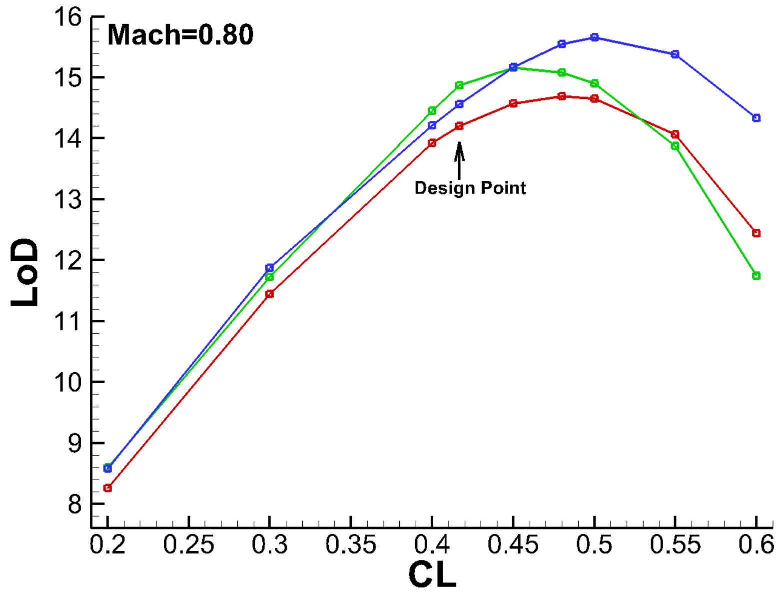

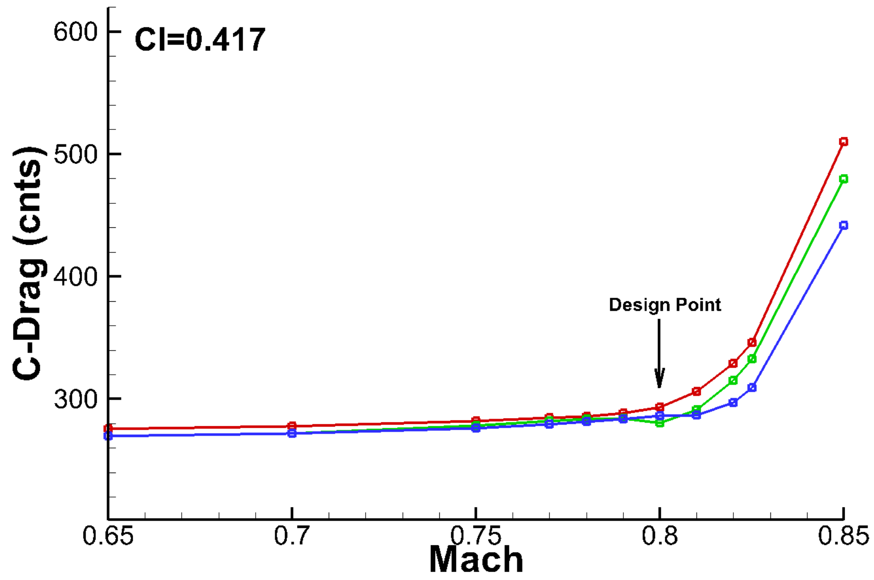

Future Work: Gradient Correction due to Trimming

- Trimming the flight with a horizontal tailplane (to reach a target pitching moment) will be considered during the Optimization.
- The gradients of our cost function need to be corrected if the flight is trimmed using horizontal tailplane. (similar to correcting gradients of drag when running for target lift).
- Use the Lagrange formulation to predict the correction term in the gradients.

Future Work: Gradient Correction due to Trimming

- Trimming the flight with a horizontal tailplane (to reach a target pitching moment) will be considered during the Optimization.
- The gradients of our cost function need to be corrected if the flight is trimmed using horizontal tailplane. (similar to correcting gradients of drag when running for target lift).
- Use the Lagrange formulation to predict the correction term in the gradients.
- If our cost function is drag then:

Correction Term

$$\frac{dC_D}{dD}@trim = \frac{C_D}{dD} + \frac{\partial C_D}{\partial \alpha_w}\left[\frac{1}{\partial C_L/\partial \alpha_w}\left(-\frac{dC_L}{dD} - \frac{\partial C_L}{\partial \alpha_t}\delta\alpha_t\right)\right] + \frac{\partial C_D}{\partial \alpha_t}\delta\alpha_t$$

$$\delta\alpha_t = \left(\frac{\partial C_{my}/\partial \alpha_w}{\partial C_L/\partial \alpha_w}\frac{dC_L}{dD} - \frac{dC_{my}}{dD}\right) / \left(\frac{\partial C_{my}}{\partial \alpha_t} - \frac{(\partial C_{my}/\partial \alpha_w)(\partial C_L/\partial \alpha_t)}{\partial C_L/\partial \alpha_w}\right)$$

α_w : far-field angle of attack

α_t : tail's angle of incidence

Future Work: Gradient Correction due to Trimming

- Tested on 2D Euler case

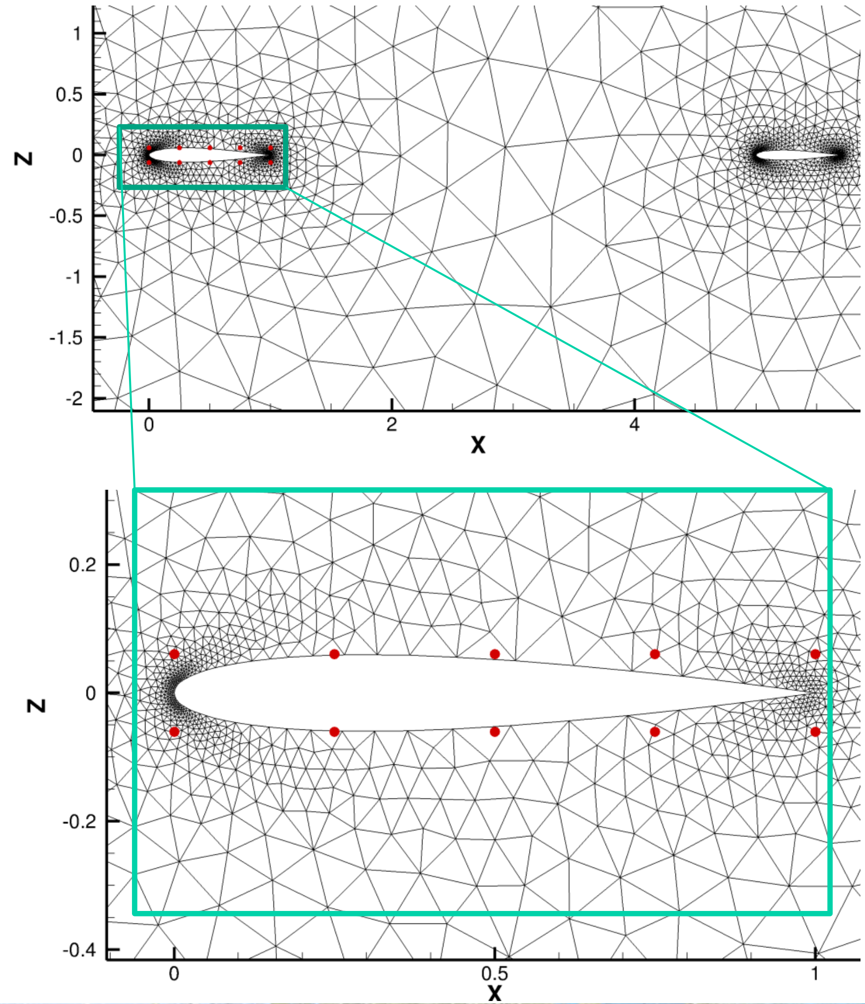

Future Work: Gradient Correction due to Trimming

- Tested on 2D Euler case

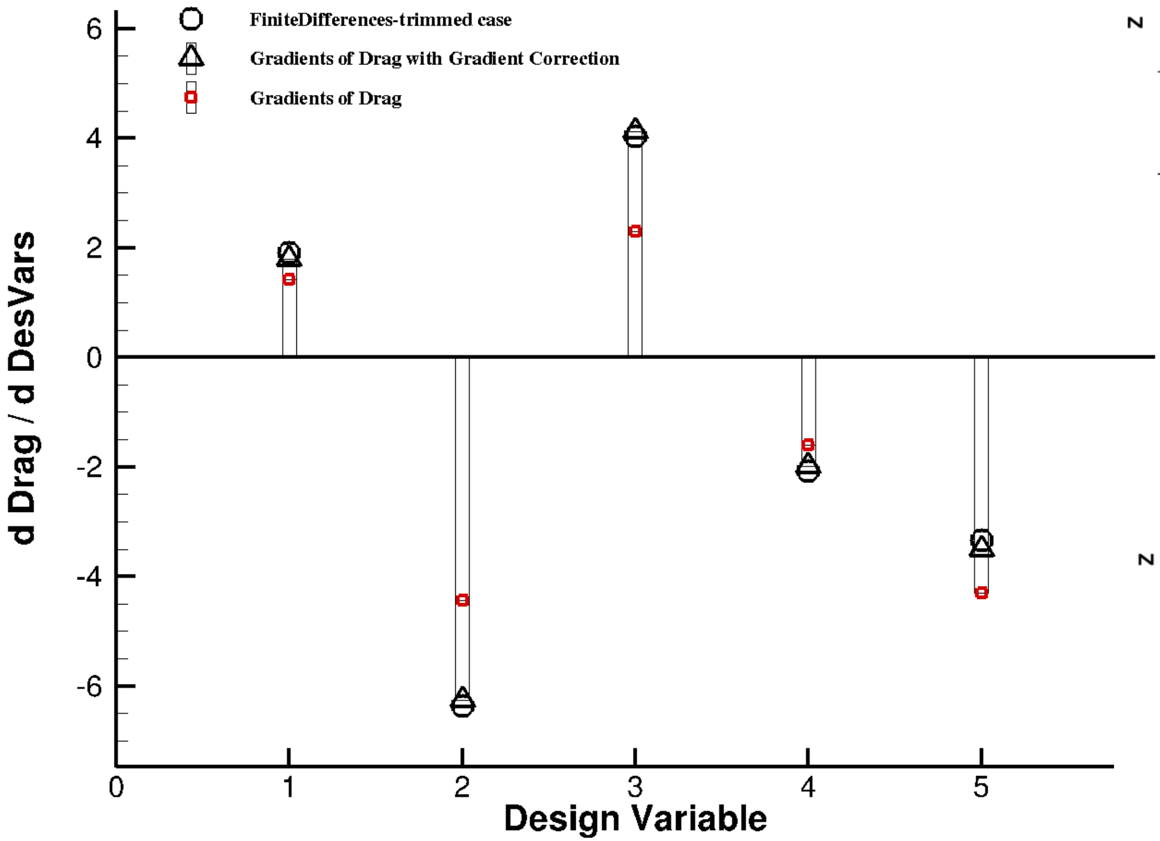

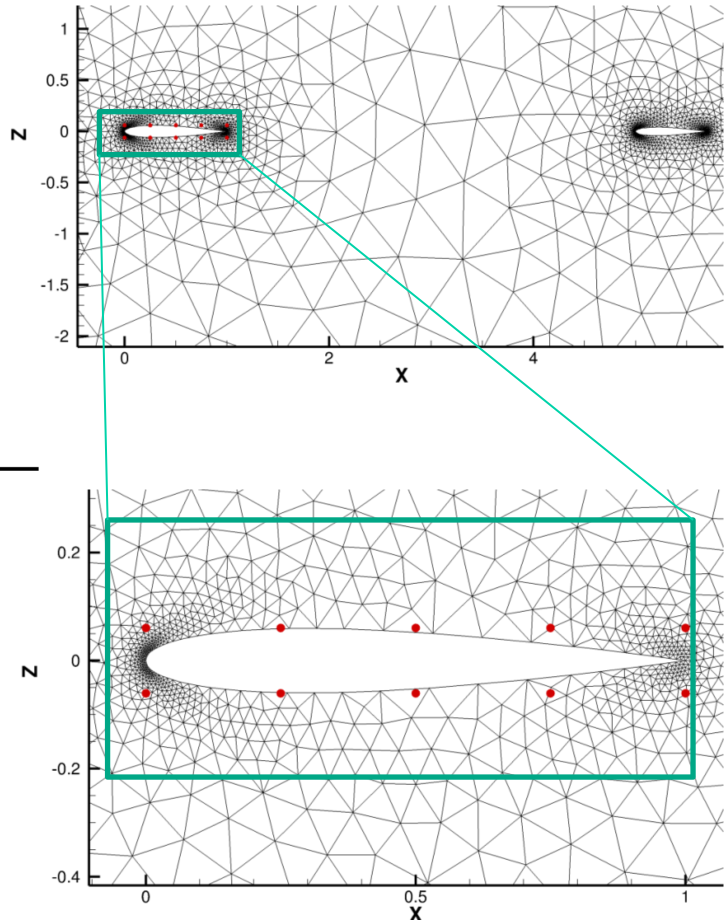

Conclusions

- The coupled aero-structural adjoint approach was employed to efficiently obtain the gradients employed in single- and multi-point aero-elastic optimizations.
- The approach employs DLR's TAU code to solve the flow equations and ANSYS Mechanical to solve the structure equations, and deals with inviscid as well as viscous turbulent flows.
- The coupled adjoint approach could save around 75% of computational time, which makes it now possible to perform aero-elastic optimizations using the gradient-based techniques, even for multi-point optimizations.
- A single- and multi-point optimizations with constrained rolling moment were performed and expected to have better effect on the structure (less weight).
- Future optimizations will include aerodynamic to structure cross sensitivities
- Future optimizations will include (horizontal tail) trimming effect

THANK YOU FOR YOUR ATTENTION